

## Supporting Information

# Aminotroponimines: ligand-centred, reversible redox events under oxidative conditions in sodium and bismuth complexes

*Anna Hanft<sup>a</sup> and Crispin Lichtenberg<sup>\*,a</sup>*

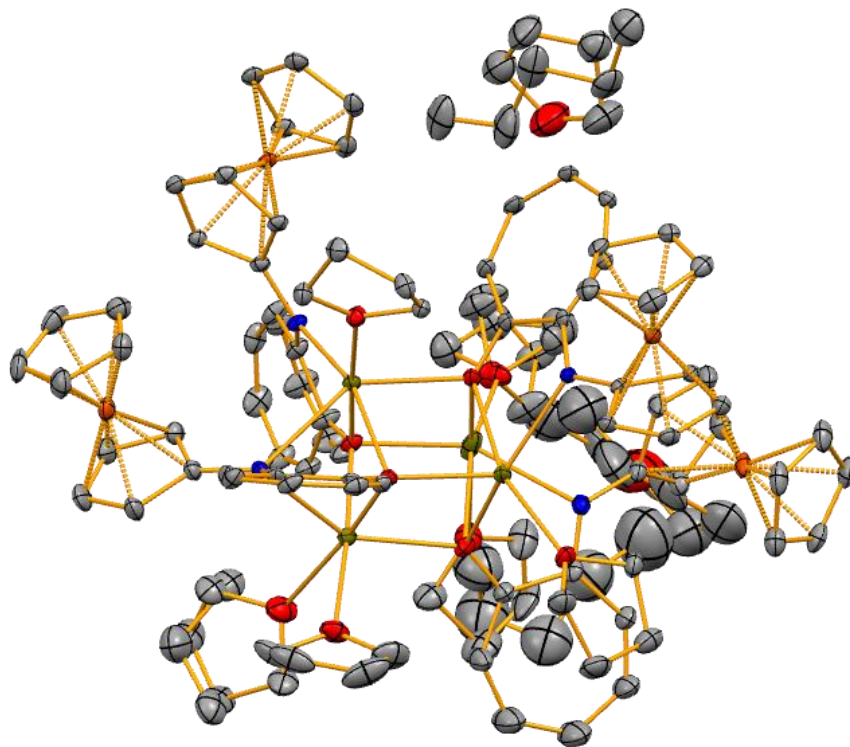
a Department of Inorganic Chemistry  
Julius-Maximilians-Universität Würzburg  
Am Hubland, 97074 Würzburg, Germany.  
Email: [crispin.lichtenberg@uni-wuerzburg.de](mailto:crispin.lichtenberg@uni-wuerzburg.de)

## Table of Contents

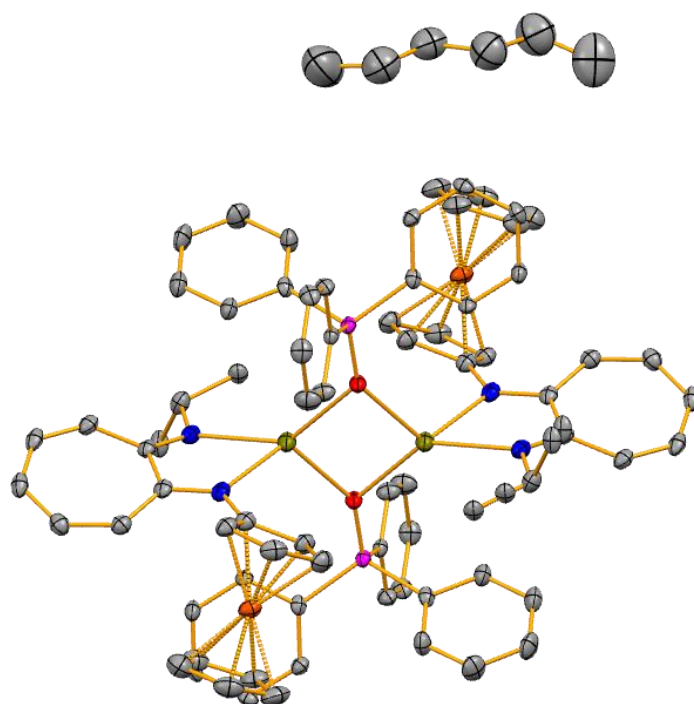
Single Crystal X-ray Analysis.....	S 02
DFT Calculations .....	S 06
Electrochemical Measurements.....	S 09
UV/vis Spectroscopy.....	S 16
NMR Spectra.....	S 17
Coordinates and Energies of Compounds Investigated by DFT Calculations.....	S 26
References.....	S 34

## Single Crystal X-ray Analysis

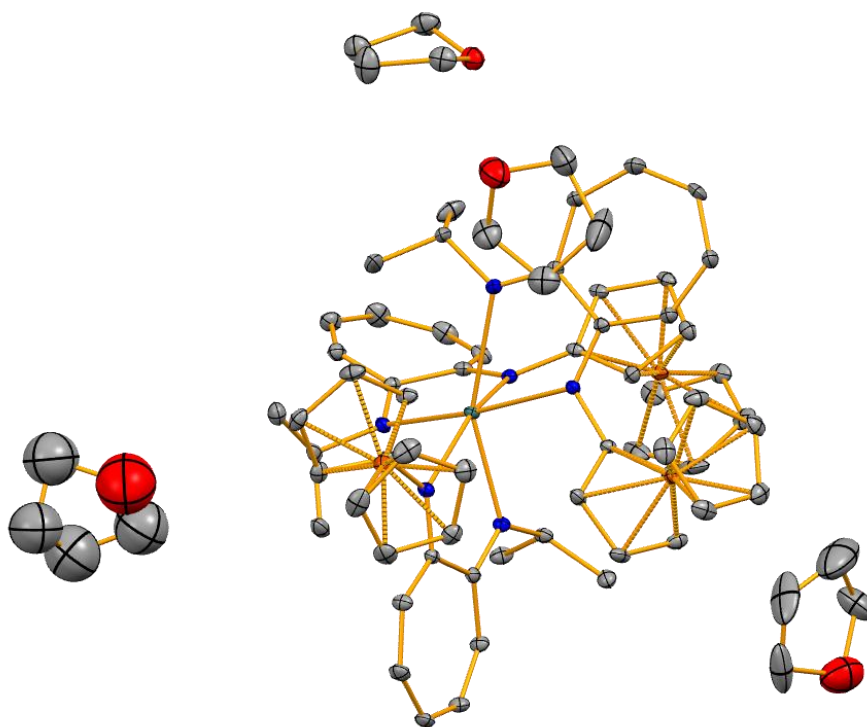
The full asymmetric units of compounds **3**·(thf)<sub>1.5</sub>, **6**-OPPh<sub>3</sub>, and **8** are not depicted in the main part, because they result in very crowded representations. They are shown in Schemes S1-S3 for completeness.



**Scheme S1.** Asymmetric unit of **3**·(thf)<sub>1.5</sub> with displacement ellipsoids shown at the 50% probability level. Hydrogen atoms are omitted for clarity.



**Scheme S2.** Asymmetric unit of **6**-OPPh<sub>3</sub> with displacement ellipsoids shown at the 50% probability level. Hydrogen atoms are omitted for clarity.



**Scheme S3.** Asymmetric unit of **8** with displacement ellipsoids shown at the 50% probability level. Hydrogen atoms are omitted for clarity.

### Solid state structure of $[\text{BiCl}_2(\text{ATI}^{\text{Fc}/i\text{Pr}})]$ (**7**).

As described in the main text, compound **7** forms a coordination polymer in the solid state, in which the repeating unit **7** shows intermolecular  $\text{Bi}\cdots\text{Cl}$  and  $\text{C}_7^{\text{ATI}}\cdots\text{C}_7^{\text{ATI}}$  interactions. A cut out of this one-dimensional coordination polymer is shown in Scheme S4a. Furthermore, every second ATI backbone (namely C1-C7) shows additional  $\text{C}_7^{\text{ATI}}\cdots\text{C}_7^{\text{ATI}}$  (arene-arene) interactions with an ATI backbone that belongs to a neighbouring polymer strand (C3-centroid<sup>ATI</sup>, 3.427(17) Å; C3-plane(C1-7), 3.346(17) Å; a centroid is defined here as the centre of an ATI ligand backbone, calculated from the positions of the seven carbon atoms C1-C7 and C21-C27, respectively.). Thus a linear double strand structure is formed in the solid state due to interaction of one ATI ligand backbone with two other ATI ligand backbones in parallel-displaced arene $\cdots$ arene bonding (Figure S4).

Bonding parameters for the description of  $\pi$ -stacking between ATI ligand backbones are summarised in Table S1.

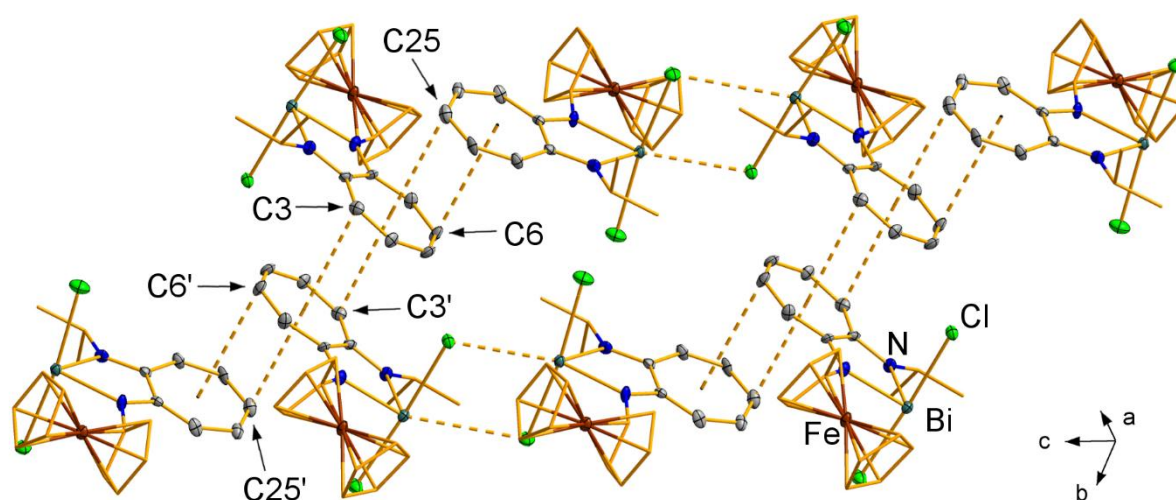


**Figure S4.** Cut out of coordination polymer (**7**)<sub>∞</sub> in the solid state.

**Table S1.** Distances for description of  $\pi$ -stacking between ATI ligand backbones in  $[\text{BiCl}_2(\text{ATI}^{\text{Fc}/i\text{Pr}})]$  (**7**).

Atom	Centroid		plane	
	ct(C1-7)	ct(C21-27)	plane(C1-7)	plane(C21-27)
C3	3.427(17) Å	-	3.346(17) Å	-
C6	-	3.758(17) Å	-	3.625(17) Å
C25	3.369(17) Å	-	3.301(17) Å	-

**Table S2.** Crystallographic data.

Data	Compound 2	Compound 3·(thf) <sub>1.5</sub>	Compound 5	Compound 6·OPPh <sub>3</sub>	Compound 7	Compound 8
Empirical formula	C <sub>17</sub> H <sub>15</sub> FeNO	C <sub>98.96</sub> H <sub>119.35</sub> Fe <sub>4</sub> N <sub>4</sub> Na <sub>4</sub> O <sub>10.27</sub>	C <sub>20</sub> H <sub>22</sub> FeN <sub>2</sub>	C <sub>88</sub> H <sub>100</sub> Fe <sub>2</sub> N <sub>4</sub> Na <sub>2</sub> O <sub>2</sub> P <sub>2</sub>	C <sub>40</sub> H <sub>42</sub> Bi <sub>2</sub> Cl <sub>4</sub> Fe <sub>2</sub> N <sub>4</sub> O <sub>2</sub> P <sub>2</sub>	C <sub>76</sub> H <sub>95</sub> BiFe <sub>3</sub> N <sub>6</sub> O <sub>4</sub>
Formula weight (g·mol <sup>-1</sup> )	305.15	1844.51	346.24	1465.33	1250.23	1533.10
Temperature (K)	101(2)	100(2)	100(2)	105(2)	101(2)	100(2)
Radiation, λ (Å)	MoK <sub>α</sub> 0.71073	MoK <sub>α</sub> 0.71073	MoK <sub>α</sub> 0.71073	MoK <sub>α</sub> 0.71073	MoK <sub>α</sub> 0.71073	MoK <sub>α</sub> 0.71073
Crystal system	Monoclinic	Triclinic	Orthorhombic	Monoclinic	Triclinic	Triclinic
Space group	<i>P</i> 12 <sub>1</sub> / <i>c</i> 1	<i>P</i> 1	<i>P</i> 2 <sub>1</sub> 2 <sub>1</sub>	<i>P</i> 1 2 <sub>1</sub> / <i>c</i> 1	<i>P</i> 1	<i>P</i> 1
<i>Unit cell dimensions</i>						
<i>a</i> (Å)	9.478(3)	15.062(3)	28.5012(14)	13.8101(5)	12.3954(8)	13.4649(19)
<i>b</i> (Å)	10.500(4)	15.807(3)	5.7094(3)	15.5735(4)	12.5471(8)	14.607(2)
<i>c</i> (Å)	13.271(5)	21.488(4)	10.1021(5)	18.4473(5)	14.5794(9)	18.529(3)
α (°)	90	85.773(6)	90	90	64.945(2)	93.978(2)
β (°)	94.603(6)	87.331(6)	90	98.746(3)	75.396(2)	107.059(2)
γ (°)	90	62.126(5)	90	90	84.677(2)	105.219(2)
Volume (Å <sup>3</sup> )	1316.5(8)	4509.9(15)	1643.86(14)	3921.4(2)	1987.5(2)	3319.2(8)
<i>Z</i>	4	2	4	2	2	2
Calculated density (mg·m <sup>-3</sup> )	1.540	1.358	1.399	1.241	2.089	1.534
Absorbption coefficient (mm <sup>-1</sup> )	1.138	0.712	0.918	0.472	9.847	3.341
<i>F</i> (000)	632	1943	728	1552	1192	1572
Theta range for collection	2.900 to 26.948°	2.328 to 25.058°	1.429 to 28.756°	2.814 to 29.182	2.253 to 26.750°	1.689 to 26.810°
Reflections collected	27828	78926	12552	27402	25022	31442
Independent reflections	2844	15892	4047	9267	8337	14110
Minimum/maximum transmission	0.5306/0.7454	0.6838/0.7452	0.6807/0.7458	0.95936/1.0000	0.6078/0.7454	0.6295/0.7461
Refinement method	Full-matrix least-squares on <i>F</i> <sup>2</sup>	Full-matrix least-squares on <i>F</i> <sup>2</sup>	Full-matrix least-squares on <i>F</i> <sup>2</sup>	Full-matrix least-squares on <i>F</i> <sup>2</sup>	Full-matrix least-squares on <i>F</i> <sup>2</sup>	Full-matrix least-squares on <i>F</i> <sup>2</sup>
Data / parameters / restraints	2844 / 185 / 0	15892 / 1321 / 486	4047 / 191 / 84	9267 / 464 / 78	8337 / 467 / 171	14110 / 825 / 104
Goodness-of-fit on <i>F</i> <sup>2</sup>	0.985	1.024	1.063	1.072	1.116	1.069
Final R indices [ <i>I</i> > 2σ( <i>I</i> )]	R <sub>1</sub> = 0.0446, wR <sup>2</sup> = 0.1115	R <sub>1</sub> = 0.0548, wR <sup>2</sup> = 0.1233	R <sub>1</sub> = 0.0970, wR <sup>2</sup> = 0.2235	R <sub>1</sub> = 0.0913, wR <sup>2</sup> = 0.2150	R <sub>1</sub> = 0.0445, wR <sup>2</sup> = 0.0852	R <sub>1</sub> = 0.0379, wR <sup>2</sup> = 0.0981
R indices (all data)	R <sub>1</sub> = 0.0666, wR <sup>2</sup> = 0.1274	R <sub>1</sub> = 0.0940, wR <sup>2</sup> = 0.1435	R <sub>1</sub> = 0.1127, wR <sup>2</sup> = 0.2314	R <sub>1</sub> = 0.1463, wR <sup>2</sup> = 0.2458	R <sub>1</sub> = 0.0689, wR <sup>2</sup> = 0.0903	R <sub>1</sub> = 0.0438, wR <sup>2</sup> = 0.1014
Maximum/minimum residual electron density (e·Å <sup>-3</sup> )	0.607 / -0.775	0.963 / -0.610	1.429 / -1.732	0.930 / -0.590	1.731 / -1.566	2.346 / -1.015

## DFT Calculations

### DFT calculations on ATI ligand H-ATI<sup>Fc/iPr</sup> (5).

Geometry optimisations of two tautomers of compound H-ATI<sup>Fc/iPr</sup> (5) in the gas phase were performed. The experimentally observed tautomer with an HNiPrR amine group (Figure S5a) was found to be lower in energy ( $H^{rel} = -2.6 \text{ kcal}\cdot\text{mol}^{-1}$ ;  $G^{rel} = -2.6 \text{ kcal}\cdot\text{mol}^{-1}$ ) than the hypothetical tautomer with an HNFCr amine group (Figure S5b).

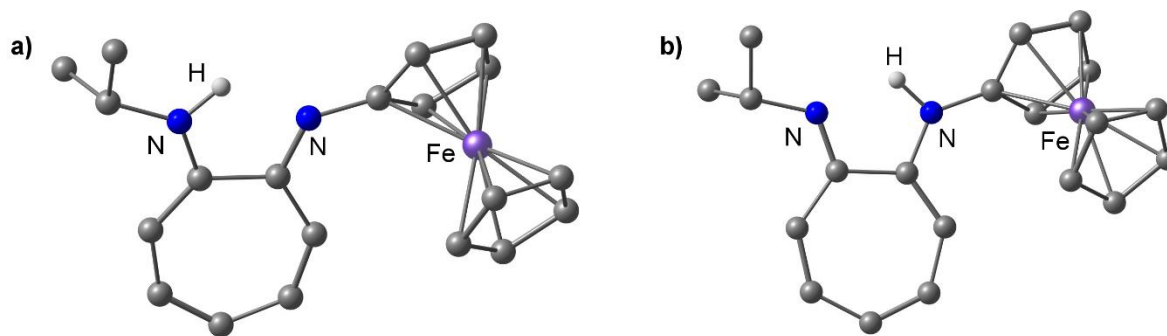


**Figure S5.** Molecular structures of two tautomers of H-ATI<sup>Fc/iPr</sup> (5) with an HNiPr amine / NFCr imine groups (a, left) or NiPr imine / HNFCr amine groups (b, right), as determined by DFT calculations. Carbon-bound hydrogen atoms are omitted for clarity.

### Spin densities of reduced and oxidised forms of AT ligand 2 and ATI ligand 5.

The spin density plots of the non-isolated radical cations [H-AT<sup>Fc</sup>]<sup>•+</sup> (2-ox) and [H-ATI<sup>Fc/iPr</sup>]<sup>•+</sup> (5-ox) as well as the non-isolated radical anions [H-AT<sup>Fc</sup>]<sup>•-</sup> (2-red) and [H-ATI<sup>Fc/iPr</sup>]<sup>•-</sup> (5-red) are shown in the main part. Further details of the spin density distributions in these species as determined by DFT calculations are given below.

**[H-AT<sup>Fc</sup>]<sup>•+</sup> (2-ox).** The Mulliken spin density for the iron atom amounts to Fe: +1.31. For all other atoms of this compound, the absolute value of the Mulliken spin densities was  $\leq 0.05$ .

**[H-AT<sup>Fc</sup>]<sup>•-</sup> (2-red).** The Mulliken spin densities for the carbon atoms in the C<sub>7</sub> backbone amount to C1: -0.07, C2: +0.36, C3: -0.11, C4: +0.24, C5: +0.12, C6: -0.01, C7: +0.32 and for the Fe atom to Fe: +0.22. For all other atoms of this compound, the absolute value of the Mulliken spin densities was  $\leq 0.03$ .

**[H-ATI<sup>Fc/iPr</sup>]<sup>•+</sup> (5-ox).** The Mulliken spin density for the iron atom amounts to Fe: +1.32. For all other atoms of this compound, the absolute value of the Mulliken spin densities was  $\leq 0.06$ .

**[H-ATI<sup>Fc/iPr</sup>]<sup>•-</sup> (5-red).** The Mulliken spin densities for the carbon atoms in the C<sub>7</sub> backbone amount to C1: -0.08, C2: +0.44, C3: -0.15, C4: +0.33, C5: +0.08, C6: +0.04, C7: +0.34. For all other atoms of this compound, the absolute value of the Mulliken spin densities was  $\leq 0.04$ .

### DFT calculations on $\text{Bi}(\text{ATI}^{\text{Fc}/i\text{Pr}})_3$ (**8**).

Geometry optimisations of two tautomers of compound  $\text{Bi}(\text{ATI}^{\text{Fc}/i\text{Pr}})_3$  (**8**) in the gas phase were performed. The experimentally observed *trans* isomer (Figure S6, left) was found to be lower in energy ( $H^{\text{rel}} = -4.1 \text{ kcal}\cdot\text{mol}^{-1}$ ;  $G^{\text{rel}} = -4.6 \text{ kcal}\cdot\text{mol}^{-1}$ ) than the *cis* isomer (Figure S6, right).

#### Optimised structures of compound **8**

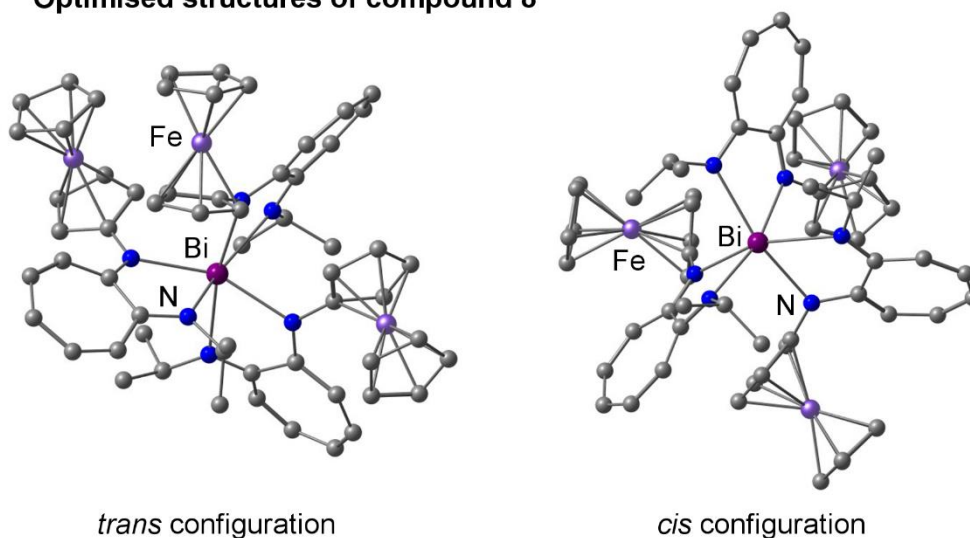


**Figure S6.** Molecular structures of  $\text{Bi}(\text{ATI}^{\text{Fc}/i\text{Pr}})_3$  (**8**) in its *trans* configuration (left) and *cis* configuration (right), as determined by DFT calculations. Hydrogen atoms are omitted for clarity.

The strongly distorted coordination geometry around the bismuth atom of **8** in its experimentally observed *trans* configuration raised the question whether the bismuth-centred lone pair might exhibit a “stereochemical activity”. A molecular orbital analysis revealed that the HOMO-9 indeed shows a significant contribution of a distorted s-type Bi centred atomic orbital, which is located between the nitrogen atoms with the largest N–Bi–N angles (Figure S7). This supports a possible “stereochemical activity” of the Bi lone pair in compound **8**.

#### HOMO-9 of compound **8** in its *trans* configuration

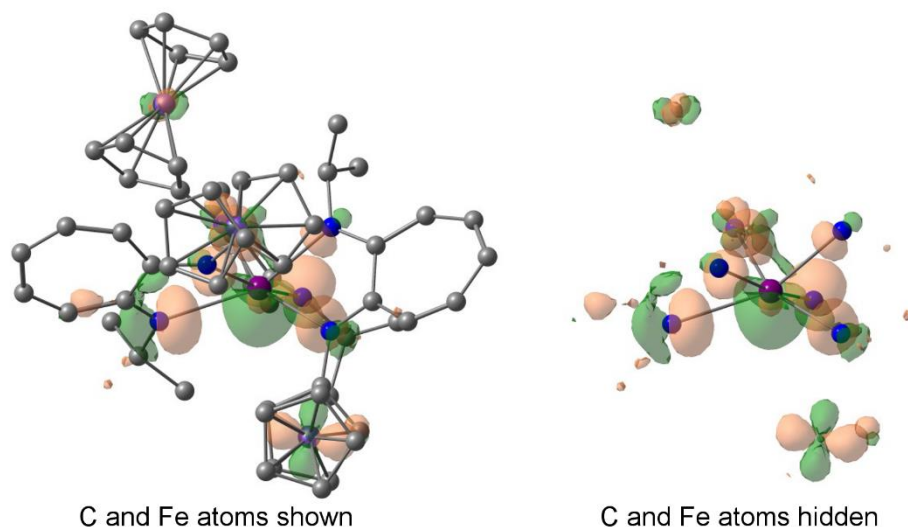


**Figure S7.** Plot of the HOMO-9 of compound **8** in its *trans* configuration with C and Fe atoms shown (left) and with C and Fe atoms omitted for clarity (right) at an isovalue of 0.04.

### DFT calculations on $[\text{Bi}(\text{AT}^{\text{Fc}})_3]^+$ ( $4^+$ ) and $[\text{Bi}(\text{ATI}^{\text{Fc}/i\text{Pr}})_3]^+$ ( $8^+$ ).

One electron oxidation of  $[\text{Bi}(\text{AT}^{\text{Fc}})_3]$  (**4**) and  $[\text{Bi}(\text{ATI}^{\text{Fc}/i\text{Pr}})_3]$  (**8**) should afford the cationic species  $[\text{Bi}(\text{AT}^{\text{Fc}})_3]^+$  ( $4^+$ ) and  $[\text{Bi}(\text{ATI}^{\text{Fc}/i\text{Pr}})_3]^+$  ( $8^+$ ). A geometry optimization and frontier orbital analysis was performed for these species. The optimized structures and singly occupied molecular orbitals (SOMOs) of  $4^+$  and  $8^+$  are shown in Figure S8. The shortest distances between the iron centres amount to 6.051 Å in  $4^+$  and to 5.796 Å in  $8^+$ .

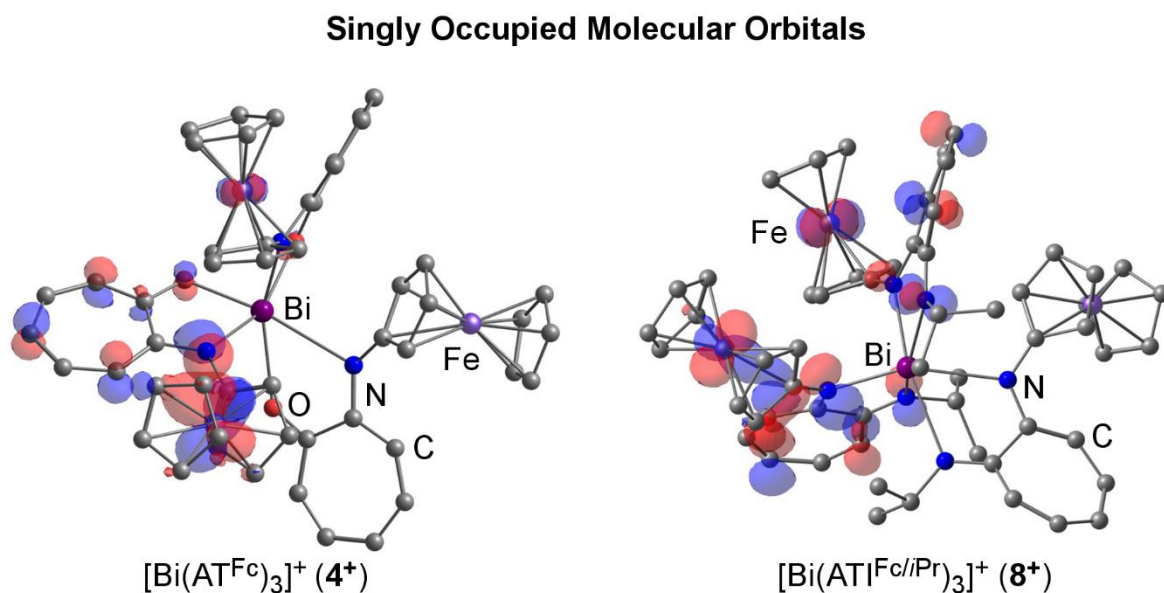


**Figure S8.** Plot of the SOMOs of compounds  $[\text{Bi}(\text{AT}^{\text{Fc}})_3]^+$  (**4**<sup>+</sup>) (left) and  $[\text{Bi}(\text{ATI}^{\text{Fc}/i\text{Pr}})_3]^+$  (**8**<sup>+</sup>) (right) at an isovalue of 0.04.



## Electrochemical Measurements

**H-AT<sup>Fc</sup> (2).** The redox wave at  $-2.38$  V is chemically reversible, when the potential window of  $-2.0$  V to  $-2.7$  V is scanned (Figure S10). When the full potential window from  $+0.50$  V to  $-3.50$  V is scanned, this redox event becomes partially reversible and a corresponding oxidation wave appears at  $-1.38$  V (Figure S9). Moreover, an irreversible reduction wave was detected at  $-3.21$  V.

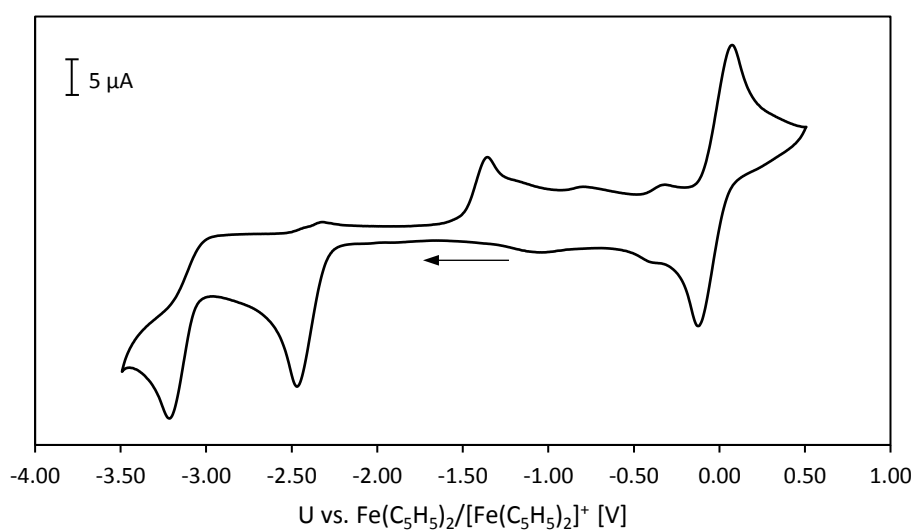


**Figure S9.** Cyclic voltammogram of **2** at 23 °C in THF / 0.1 M  $[N(nBu)_4][PF_6]$  at a scan rate of  $250 \text{ mV}\cdot\text{s}^{-1}$ .

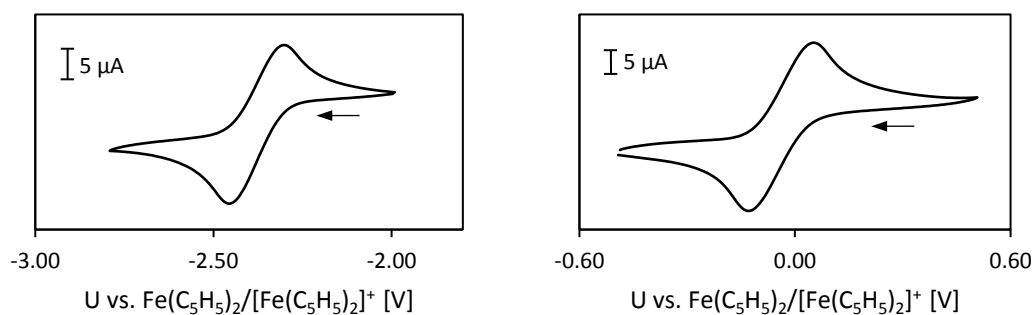


**Figure S10.** Cyclic voltammograms of **2** at 23 °C in THF / 0.1 M  $[N(nBu)_4][PF_6]$  at scan rates of  $250 \text{ mV}\cdot\text{s}^{-1}$  for two different potential windows.

**Na(AT<sup>Fe</sup>)<sub>3</sub> (3).**

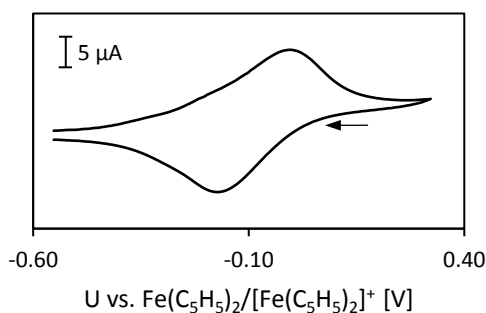


**Figure S11.** Cyclic voltammogram of **3** at 23 °C in THF / 0.1 M [N(*n*Bu)<sub>4</sub>][PF<sub>6</sub>] at a scan rate of 250 mV·s<sup>-1</sup>.

**Bi(AT<sup>Fe</sup>)<sub>3</sub> (4).**

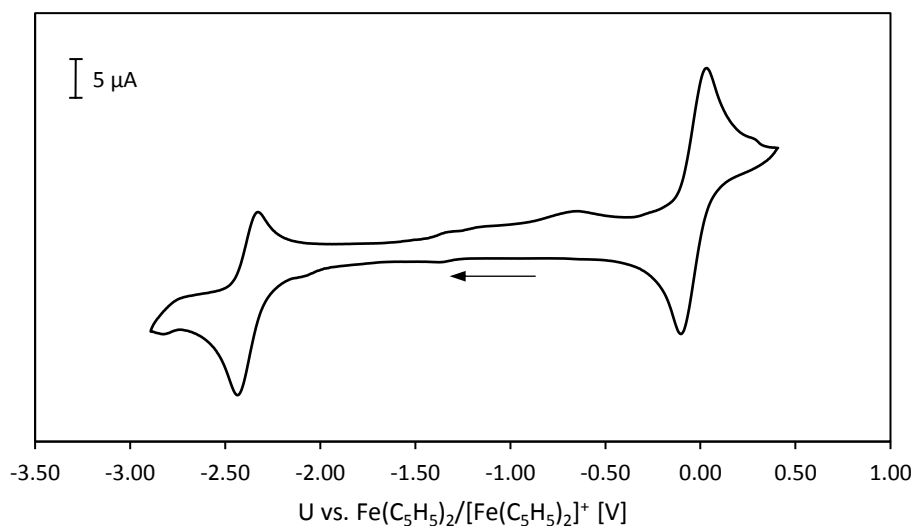


**Figure S12.** Cyclic voltammogram of **4** at 23 °C in THF / 0.1 M [N(*n*Bu)<sub>4</sub>][PF<sub>6</sub>] at a scan rate of 250 mV·s<sup>-1</sup>.

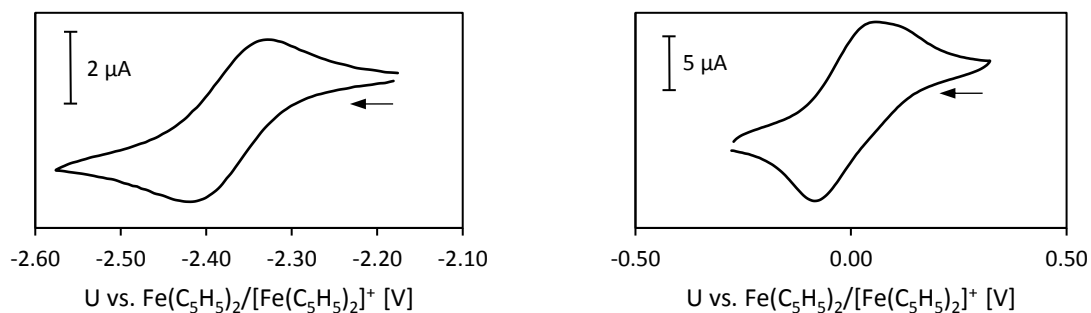


**Figure S13.** Cyclic voltammogram of **4** at 23 °C in THF / 0.1 M [N(*n*Bu)<sub>4</sub>][PF<sub>6</sub>] at scan rates of 250 mV·s<sup>-1</sup>.

**H-ATl<sup>Fc/iPr</sup> (5).** The redox wave at  $-2.64$  V is chemically reversible, when the potential window of  $-2.0$  V to  $-2.5$  V is scanned (Figure S15). When the full potential window from  $+0.30$  V to  $-3.50$  V is scanned, this redox event becomes partially reversible and a corresponding oxidation wave appears at  $-1.63$  V (Figure S14).

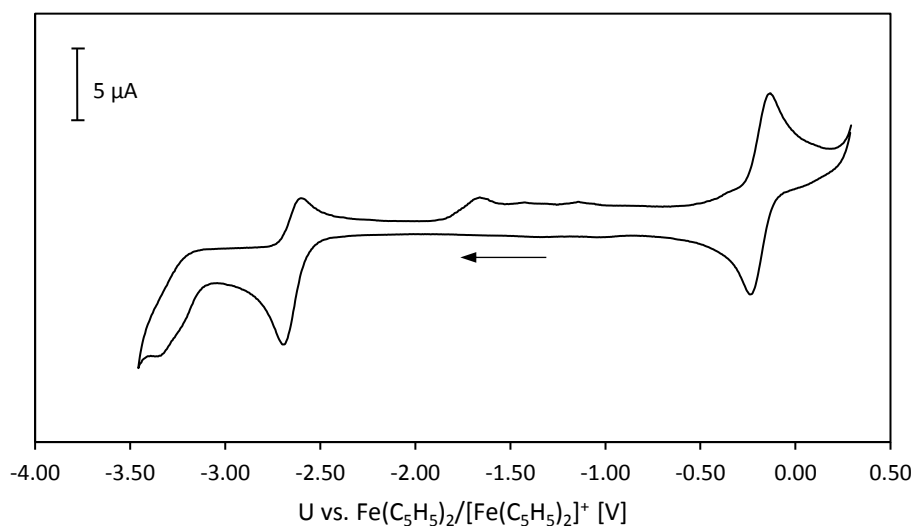


**Figure S14.** Cyclic voltammogram of **5** at  $23$  °C in THF /  $0.1$  M  $[N(nBu)_4][PF_6]$  at a scan rate of  $250$   $mV \cdot s^{-1}$ .

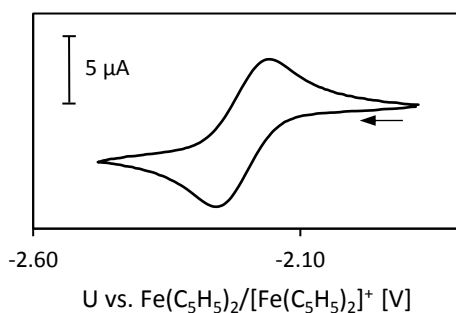


**Figure S15.** Cyclic voltammogram of **5** at  $23$  °C in THF /  $0.1$  M  $[N(nBu)_4][PF_6]$  at a scan rate of  $250$   $mV \cdot s^{-1}$ .

**[Na(ATI<sup>Fe/iPr</sup>)(OPPh<sub>3</sub>)] (6-OPPh<sub>3</sub>).** In addition to the redox events described in the main part of this document, a chemically reversible redox event was detected at potentials of  $-3.07$  V, where beginning solvent decomposition can play a role (Figure S16).

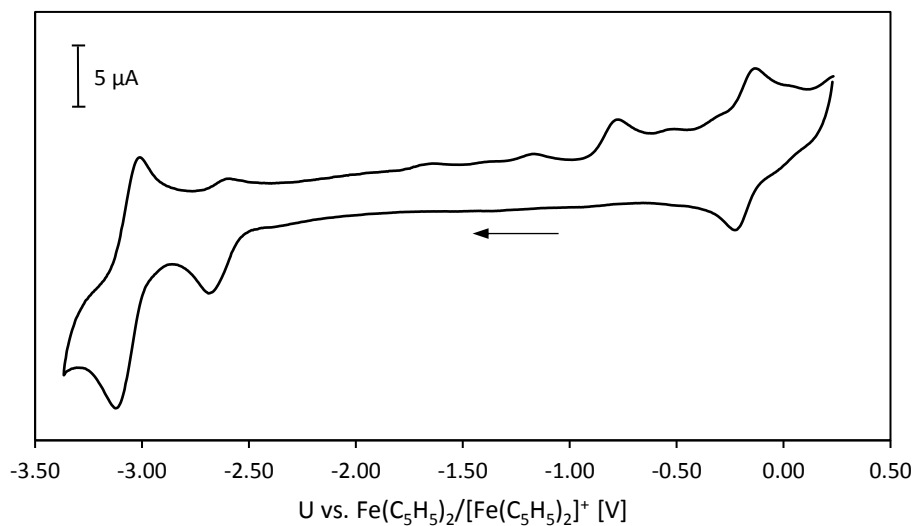


**Figure S16.** Cyclic voltammogram of **6-OPPh<sub>3</sub>** at 23 °C in THF / 0.1 M [N(*n*Bu)<sub>4</sub>][PF<sub>6</sub>] at a scan rate of 250 mV·s<sup>-1</sup>.

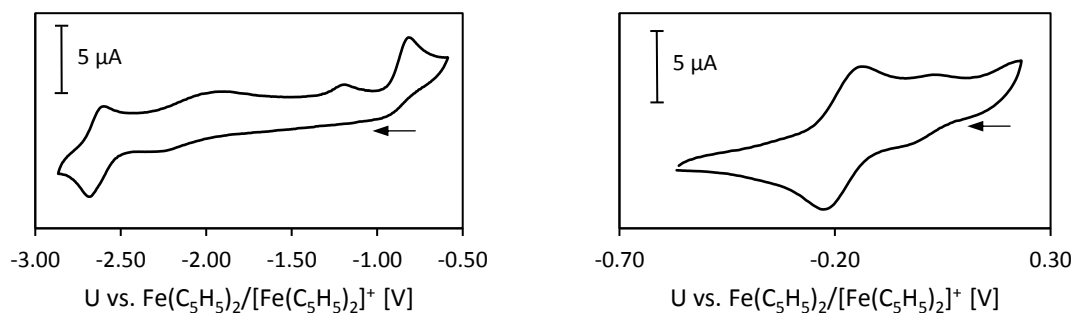


**Figure S17.** Cyclic voltammogram of **6-OPPh<sub>3</sub>** at 23 °C in THF / 0.1 M [N(*n*Bu)<sub>4</sub>][PF<sub>6</sub>] at scan rates of 250 mV·s<sup>-1</sup>.

**Bi(ATI<sup>Fe/Pr</sup>)Cl<sub>2</sub> (7).** In addition to the redox events discussed in the main part, a redox event was detected at  $-2.67$  V. The nature of the species associated with this redox event is not discussed due to the ill-defined redox events that take place at  $-1.08$  V and  $-1.31$  V.

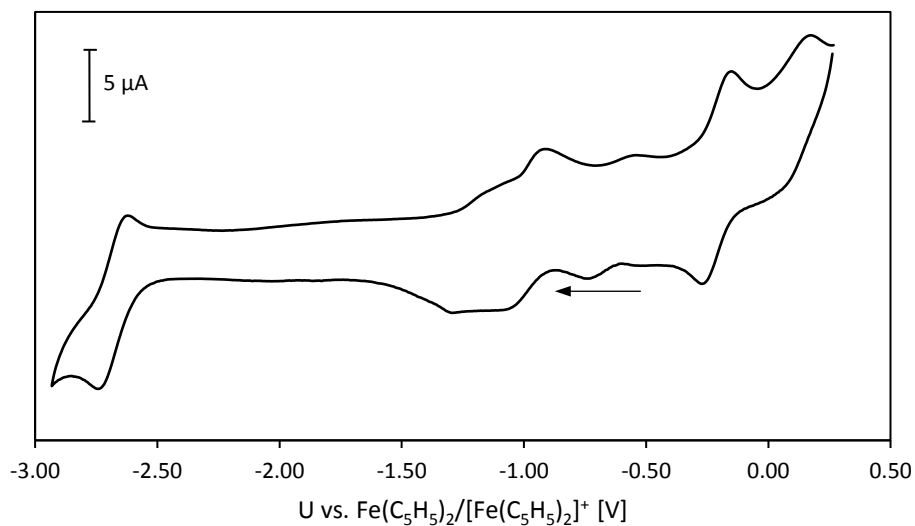


**Figure S18.** Cyclic voltammogram of **7** at 23 °C in THF / 0.1 M [N(*n*Bu)<sub>4</sub>][PF<sub>6</sub>] at a scan rate of 250 mV·s<sup>-1</sup>.

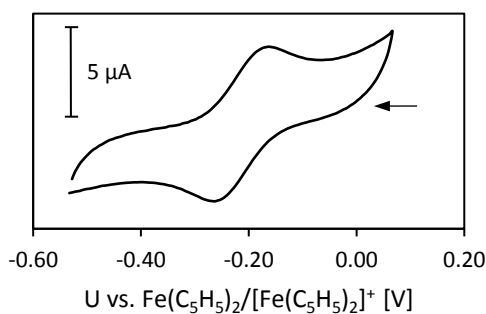


**Figure S19.** Cyclic voltammogram of **7** at 23 °C in THF / 0.1 M [N(*n*Bu)<sub>4</sub>][PF<sub>6</sub>] at a scan rate of 250 mV·s<sup>-1</sup>.

**Bi(ATI<sup>Fe/iPr</sup>)<sub>3</sub> (8).**

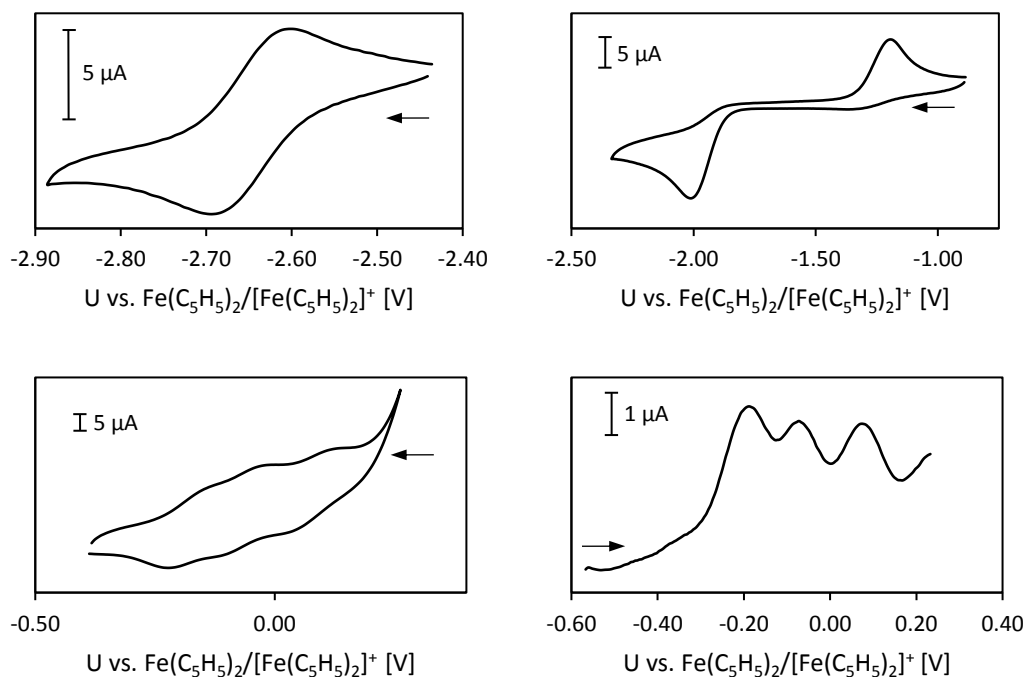


**Figure S20.** Electrochemical measurements of **8** at 23 °C in THF / 0.1 M [N(*n*Bu)<sub>4</sub>][PF<sub>6</sub>]. Top row and bottom left: cyclic voltammograms at scan rates of 250 mV·s<sup>-1</sup>. Bottom right: differential pulse voltammogram with step size of 5 mV, pulse size of 25 mV, sample period of 0.2 s and pulse time of 0.1 s.

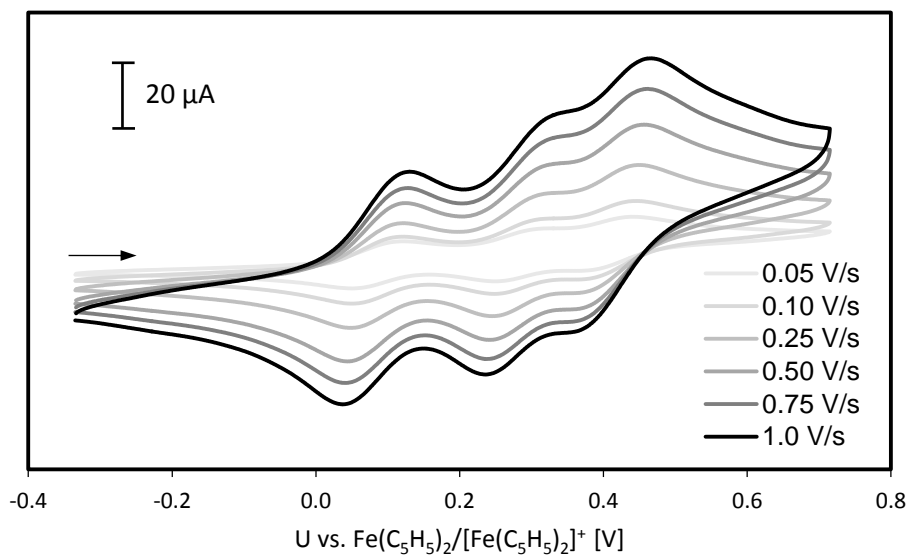


**Figure S21.** Cyclic voltammogram of **8** at 23 °C in CH<sub>2</sub>Cl<sub>2</sub> / 0.1 M [N(*n*Bu)<sub>4</sub>][PF<sub>6</sub>] at scan rates ranging from 50 to 1000 mV·s<sup>-1</sup>.

A plot of the square root of the anodic peak current vs. the scan rate is shown for the redox event at  $-0.23$  V as a representative example for results obtained from cyclic voltammograms of **8** at  $23$  °C in  $\text{CH}_2\text{Cl}_2 / 0.1$  M  $[\text{N}(n\text{Bu})_4][\text{PF}_6]$  (Figure S22).

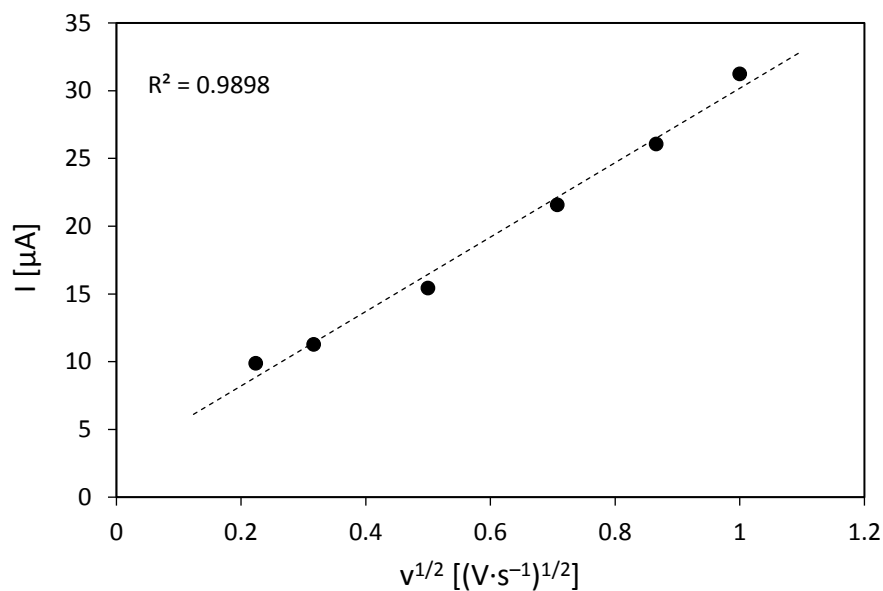


**Figure S22.** Plot of anodic peak current vs. square root of scan rate for the redox event at  $-0.23$  V in cyclic voltammograms of **8** at  $23$  °C in  $\text{CH}_2\text{Cl}_2 / 0.1$  M  $[\text{N}(n\text{Bu})_4][\text{PF}_6]$ .

## UV/vis spectroscopy

The coloured compounds **2-8** were investigated by UV/vis spectroscopy in THF solution. The starting material  $\text{H}_2\text{NFc}$  shows a broad absorption band at 442 nm. This band is shifted to 476 nm, 500 nm, and 482 nm for compounds **2**, **3**, and **4**, respectively (Figure S23). The aminotroponates show two additional absorption maxima, which could thus be ascribed to the presence of the troponate moiety. These maxima are similar for the free ligand **2** (346 nm, 409 nm) and the bismuth compound **4** (348 nm, 410 nm) and red-shifted for the sodium compound **3** (415 nm, 500 nm).

For the aminotroponimate compounds **5-8**, the UV-vis spectra show features in the range of 360-410 nm and 420-510 nm, some of which consist of more than one individual band (Figure S24). The bismuth compounds and the free ligand show considerable similarities with respect to intensity and wavelength of the maxima. For the sodium compounds, the bands in the range of 420-510 nm exhibit higher intensities.

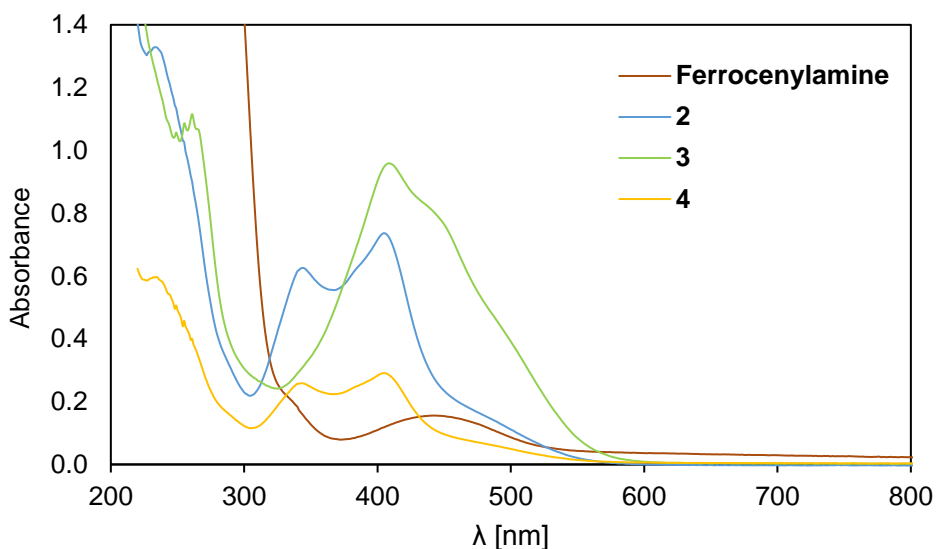


**Figure S23.** UV-vis spectra of compounds **2**, **3**, **4**, and  $\text{H}_2\text{NFc}$  in THF.

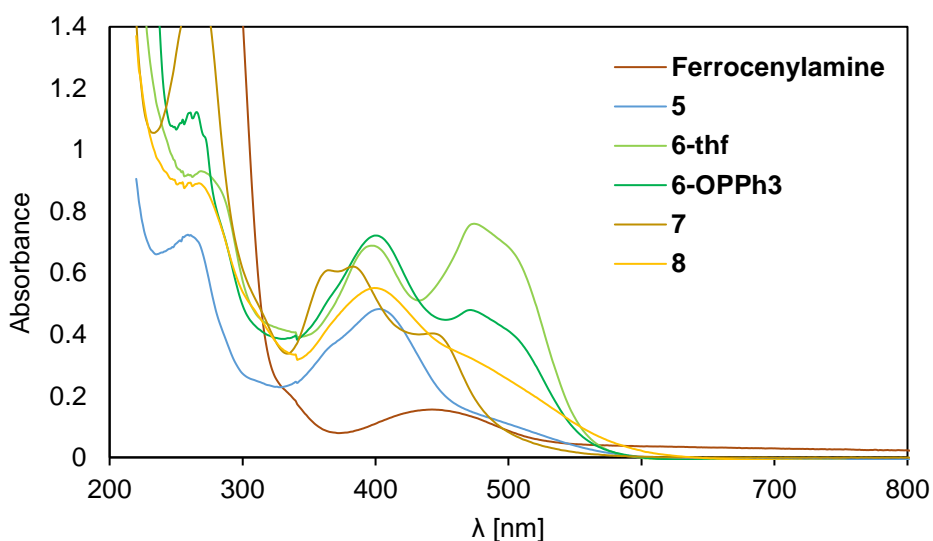


**Figure S24.** UV-vis spectra of compounds **5**, **6-thf**, **6-OPPh3**, **7**, **8**, and  $\text{H}_2\text{NFc}$  in THF.



# NMR Spectra

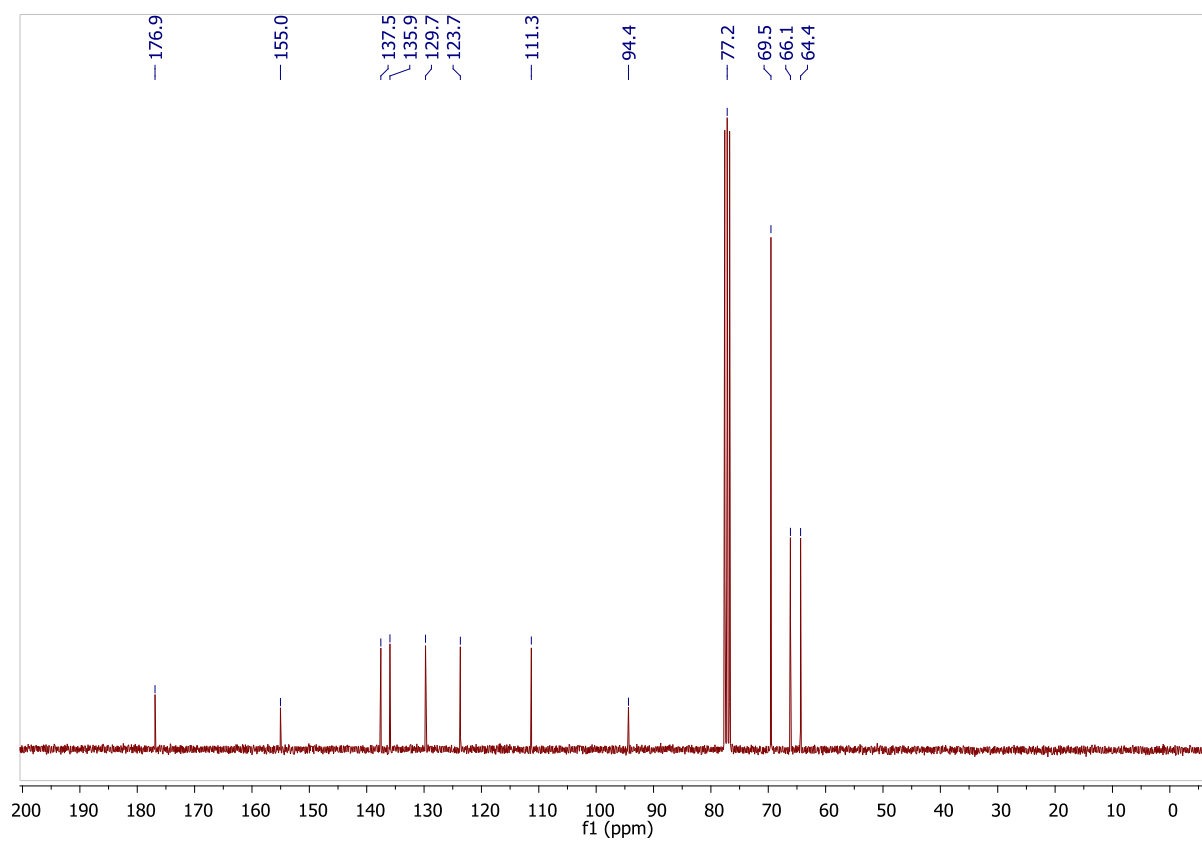
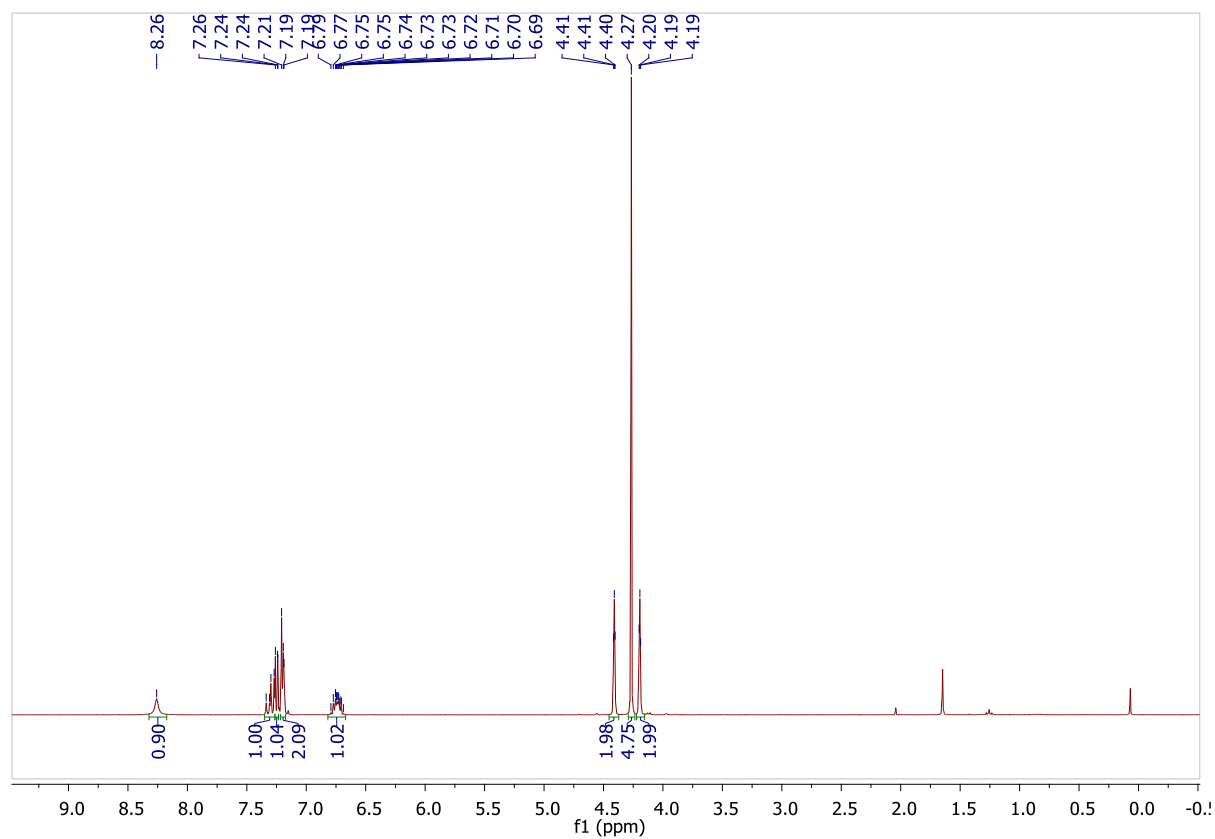
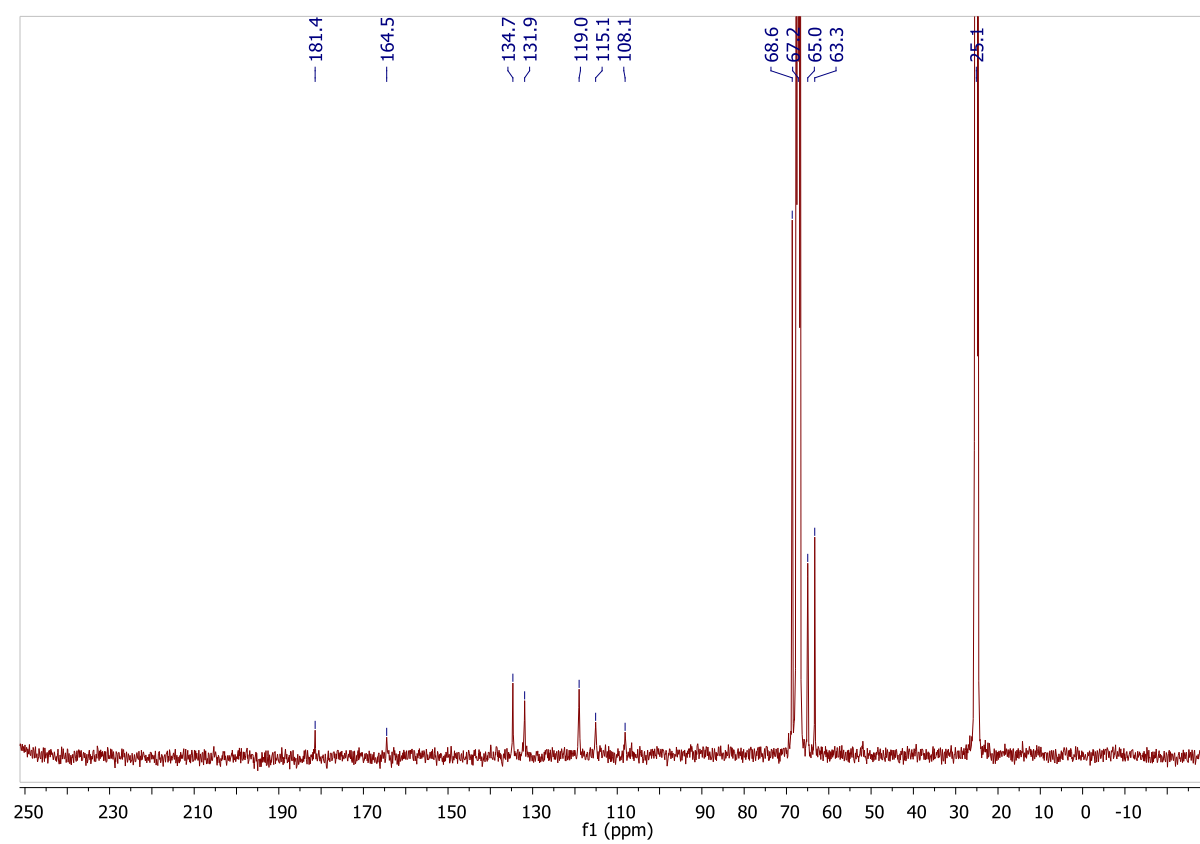
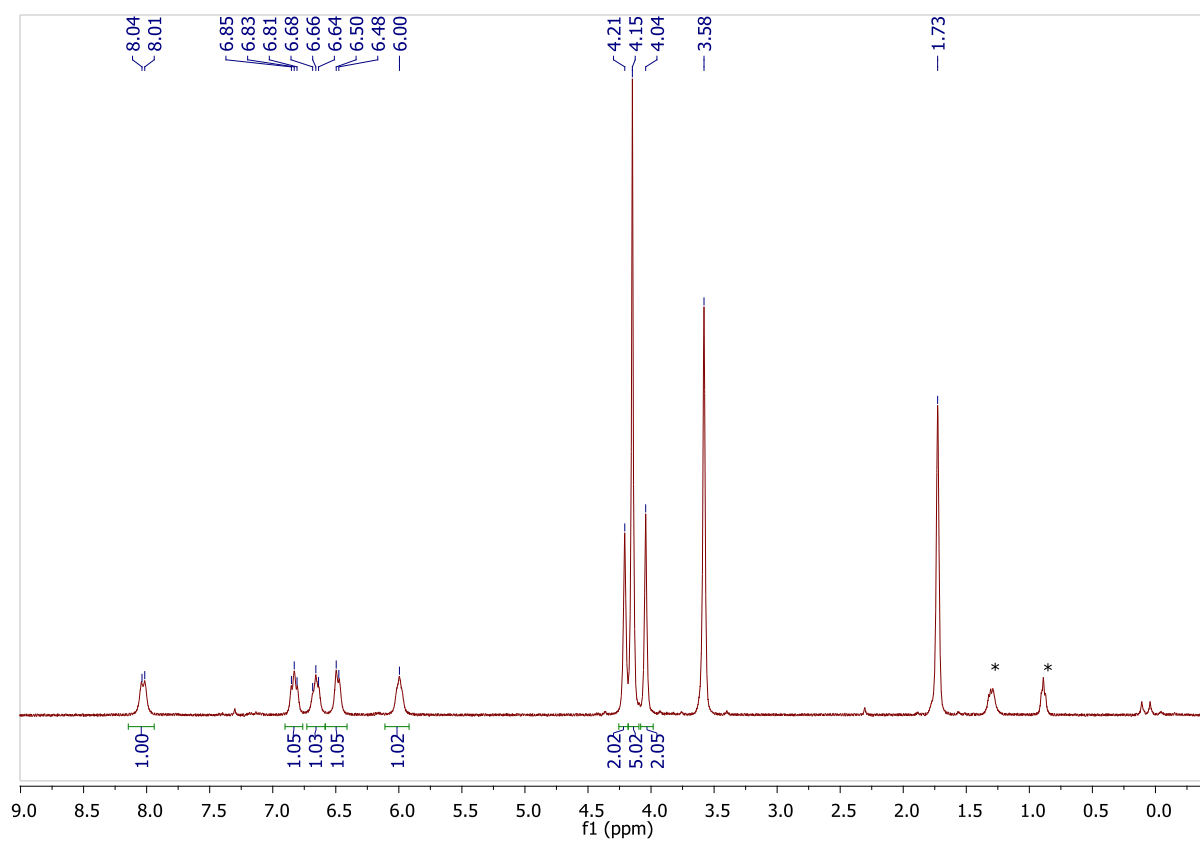
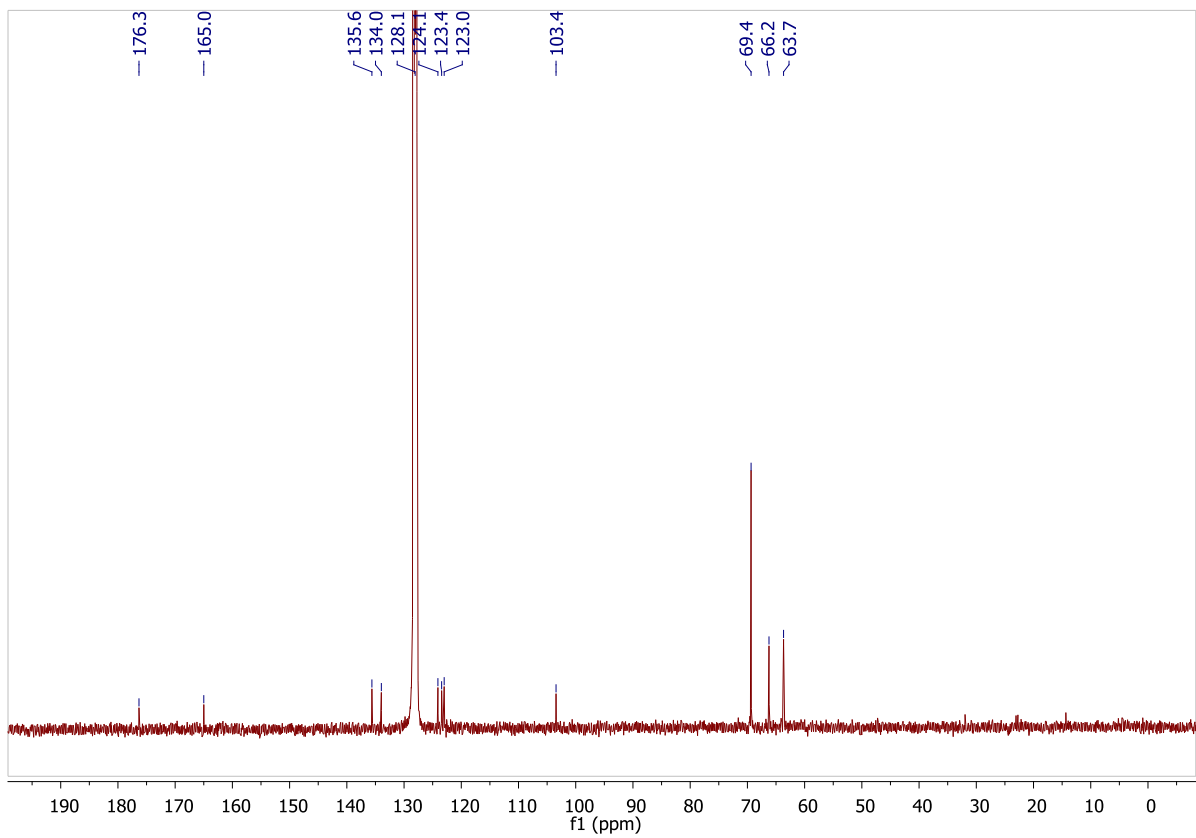
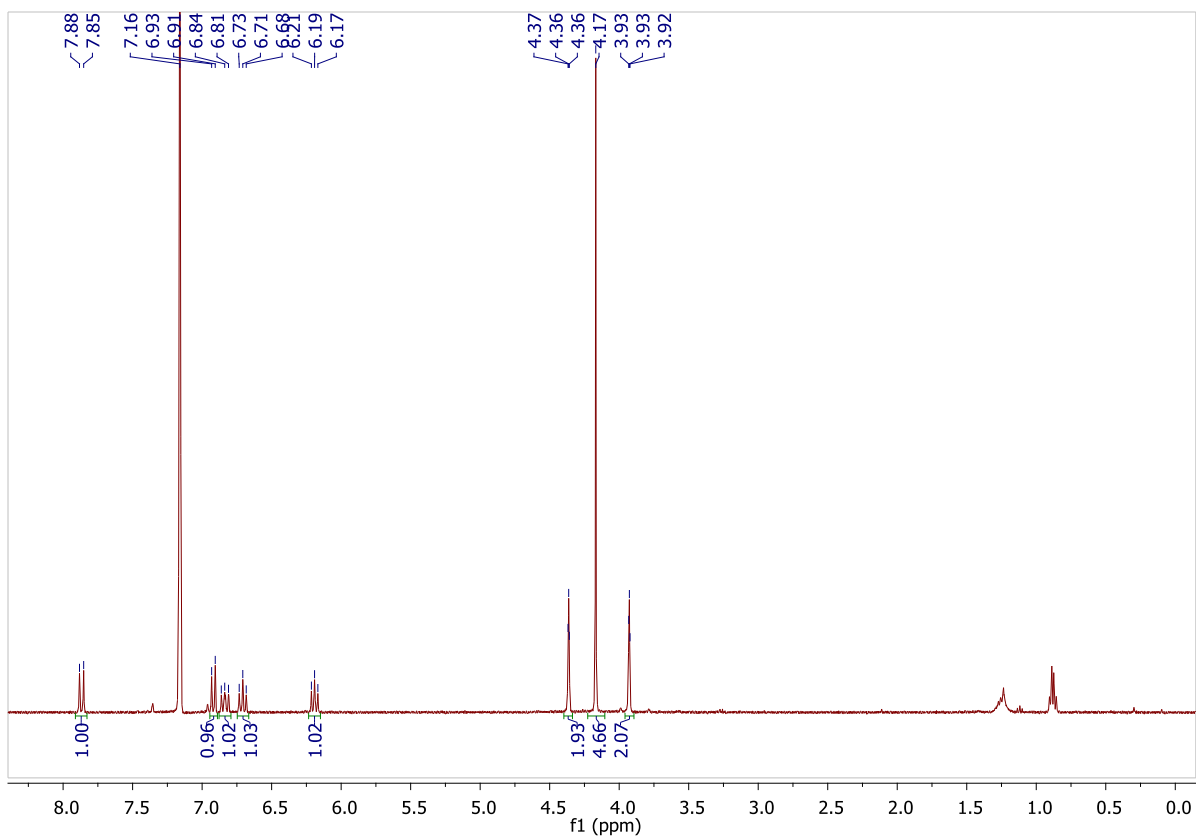


Figure S25.  $^1\text{H}$  and  $^{13}\text{C}$  NMR spectra of **2** in  $\text{CDCl}_3$ .



**Figure S26.**  $^1\text{H}$  and  $^{13}\text{C}$  NMR spectra of **3** in  $\text{THF-}d_8$ ; asterisks denote resonances due to residual amounts of hexanes.



**Figure S27.**  $^1\text{H}$  and  $^{13}\text{C}$  NMR spectra of **4** in  $\text{C}_6\text{D}_6$ .

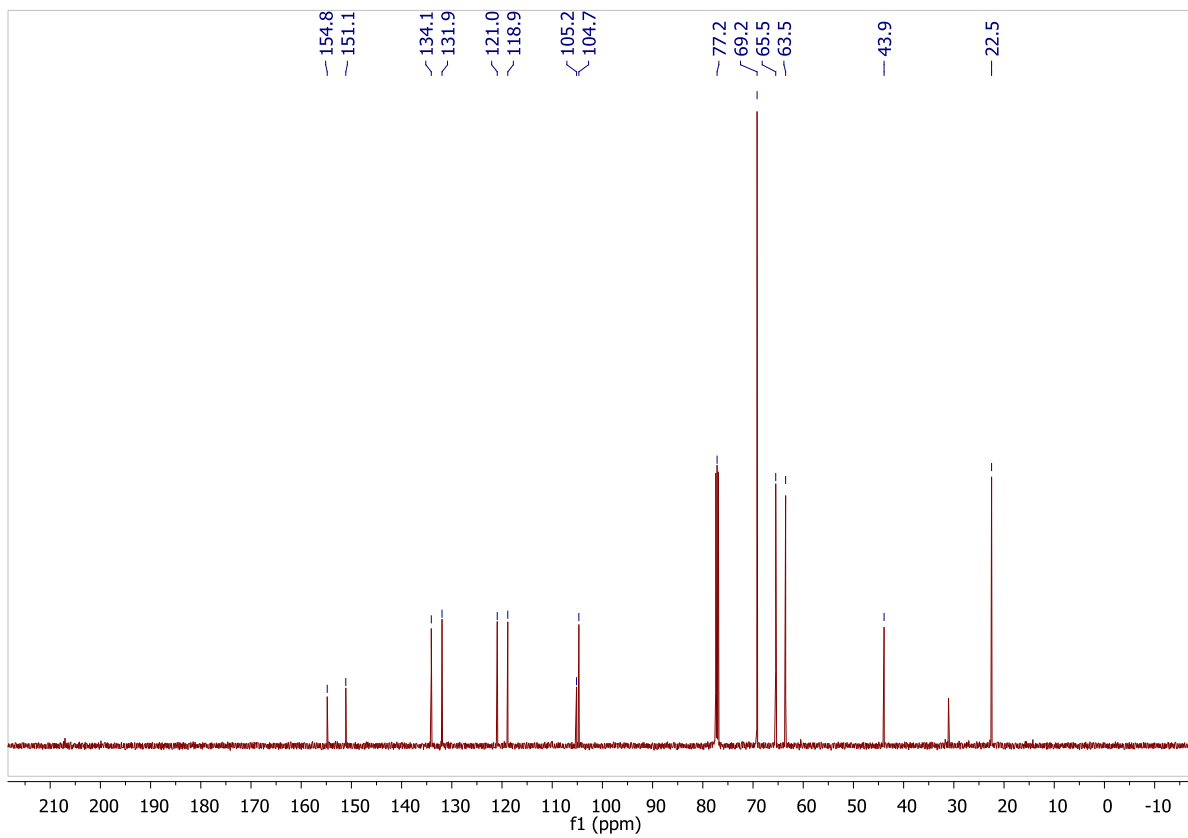
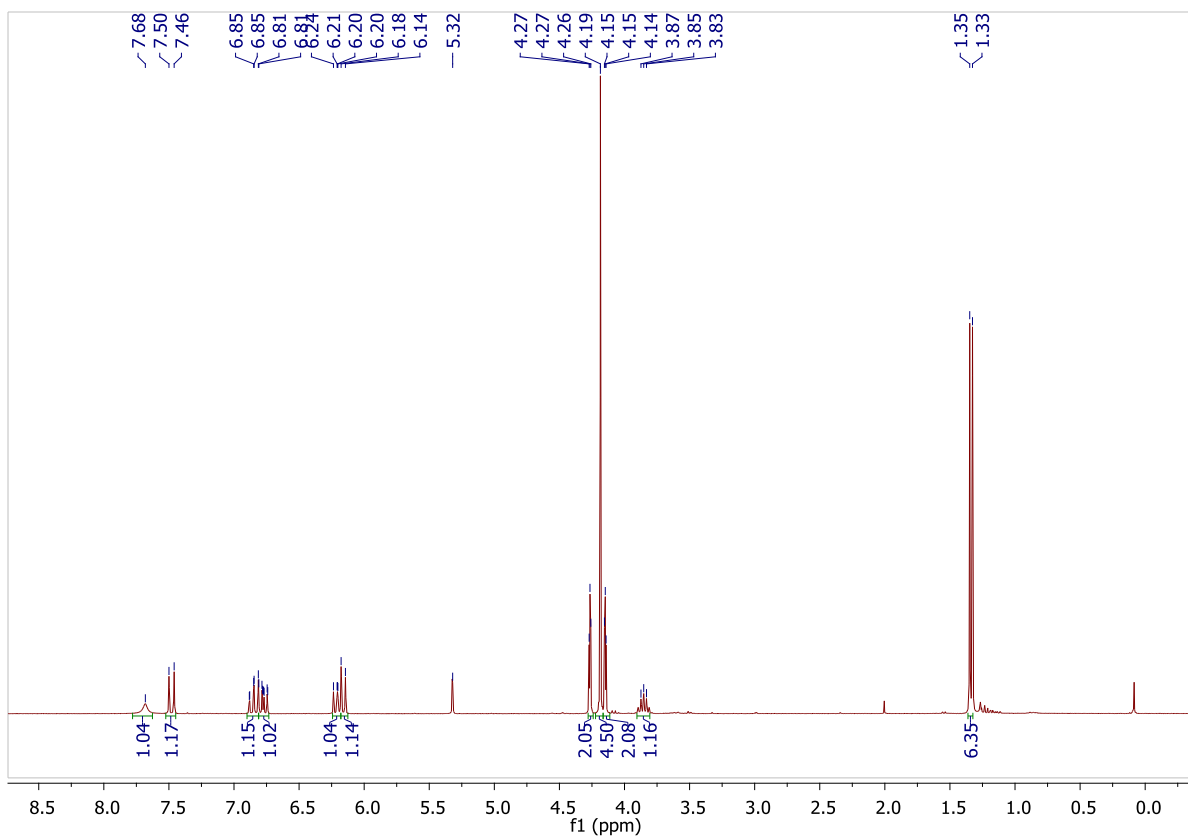


**Figure S28.** <sup>1</sup>H and <sup>13</sup>C NMR spectra of **5** in CD<sub>2</sub>Cl<sub>2</sub> and CDCl<sub>3</sub>, respectively.

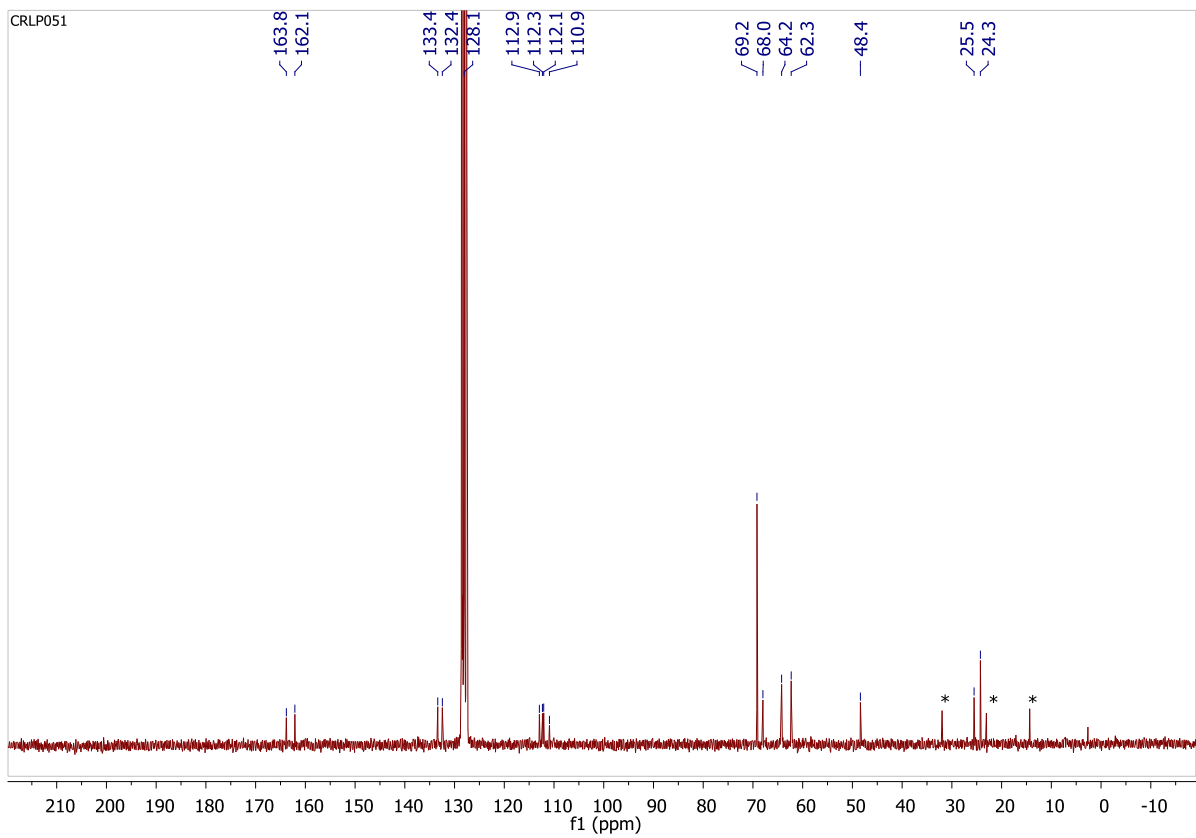
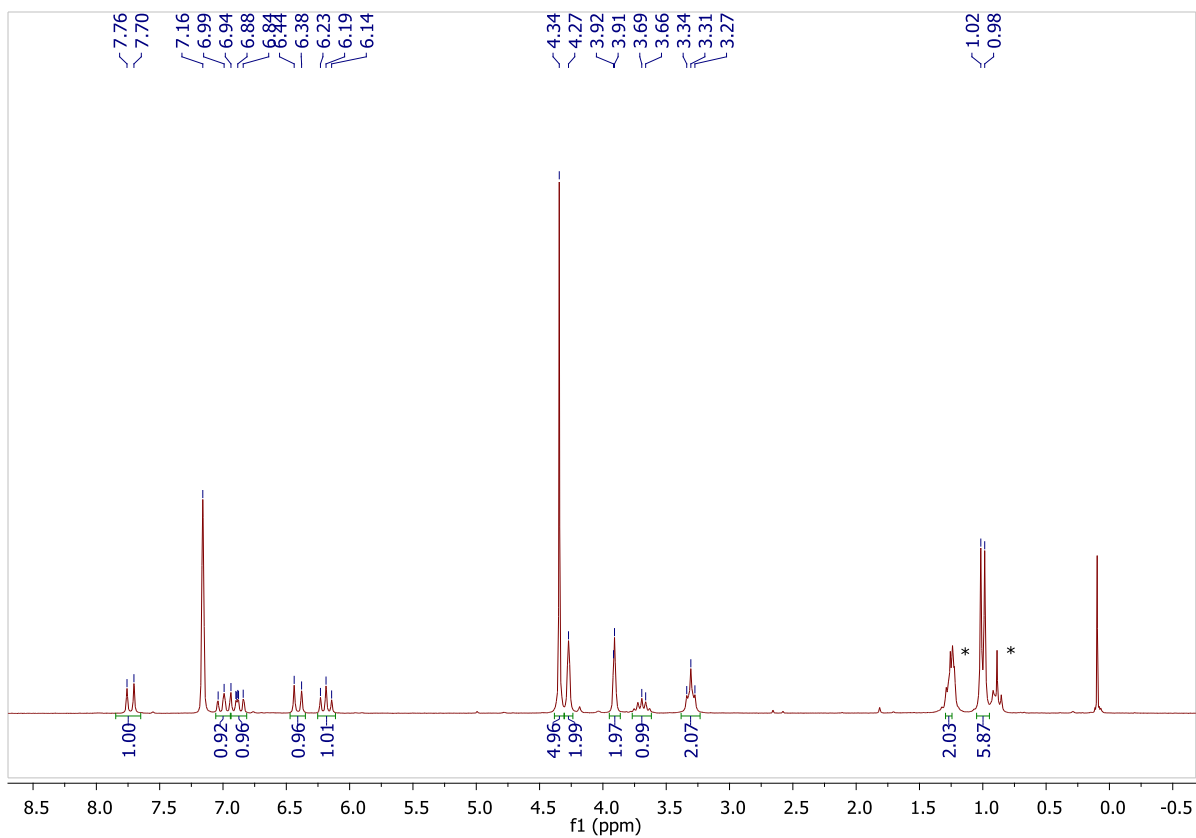


**Figure S29.**  $^1\text{H}$  and  $^{13}\text{C}$  NMR spectra of **6-thf** in  $\text{C}_6\text{D}_6$ ; asterisks denote residual amounts of hexanes.

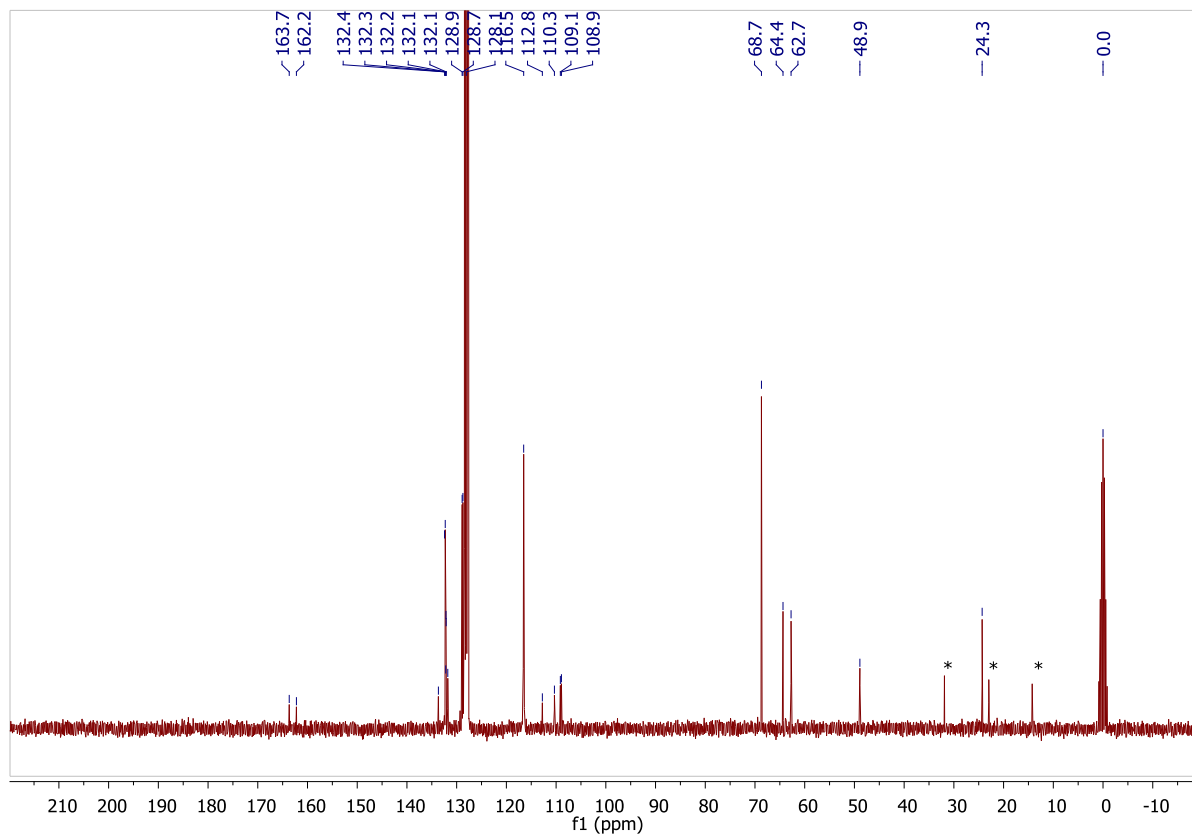
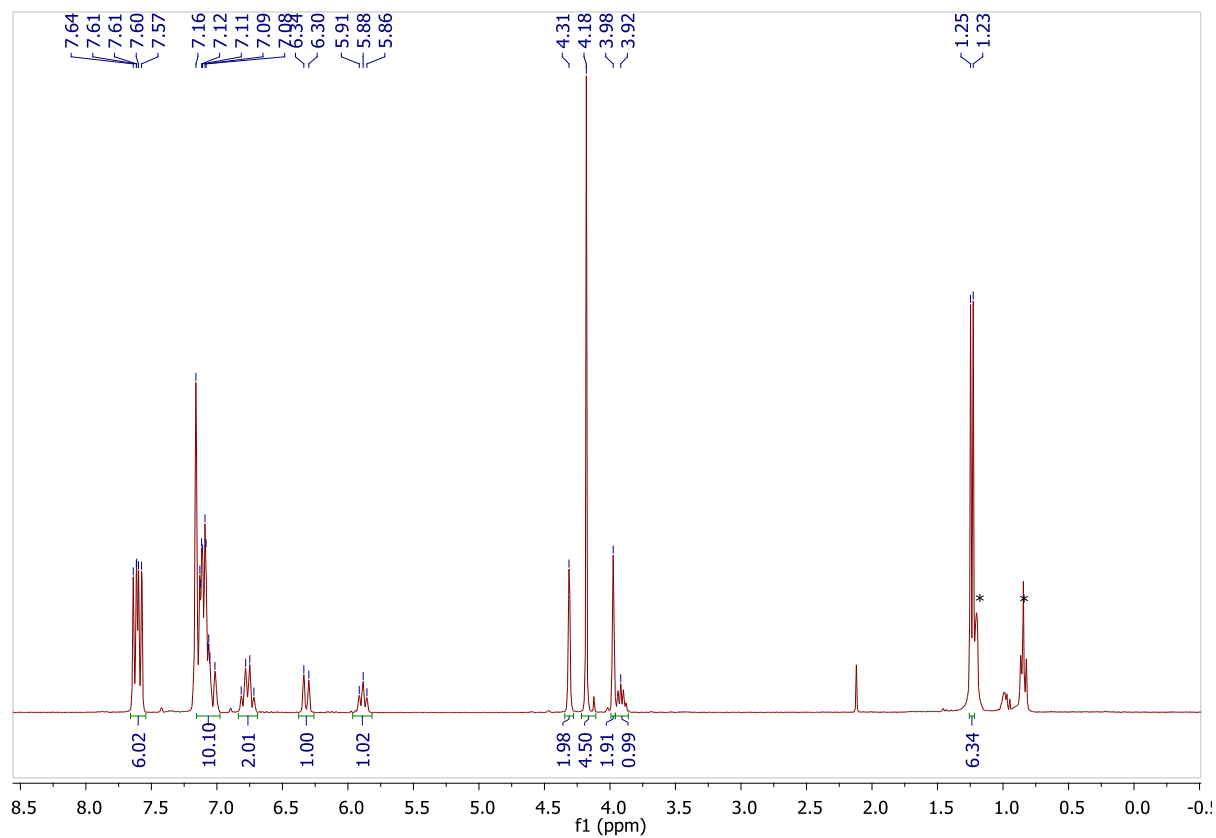


**Figure S30.**  $^1\text{H}$  and  $^{13}\text{C}$  NMR spectra of **6-OPPh<sub>3</sub>** in  $\text{C}_6\text{D}_6/\text{MeCN-}d_3$  (10:1); asterisks denote residual amounts of hexanes.

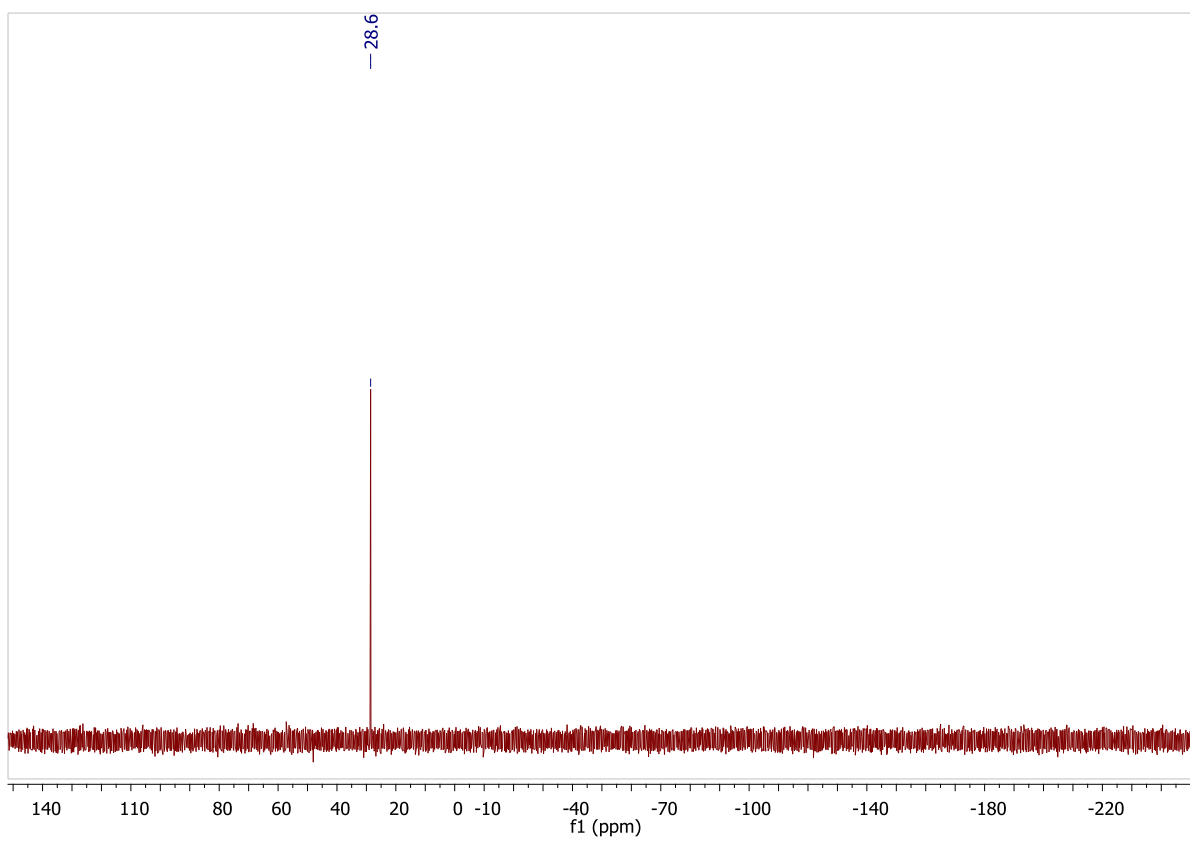


**Figure S31.**  $^{31}\text{P}$  NMR spectrum of **6-OPPh<sub>3</sub>** in  $\text{C}_6\text{D}_6/\text{MeCN-}d_3$  (10:1).

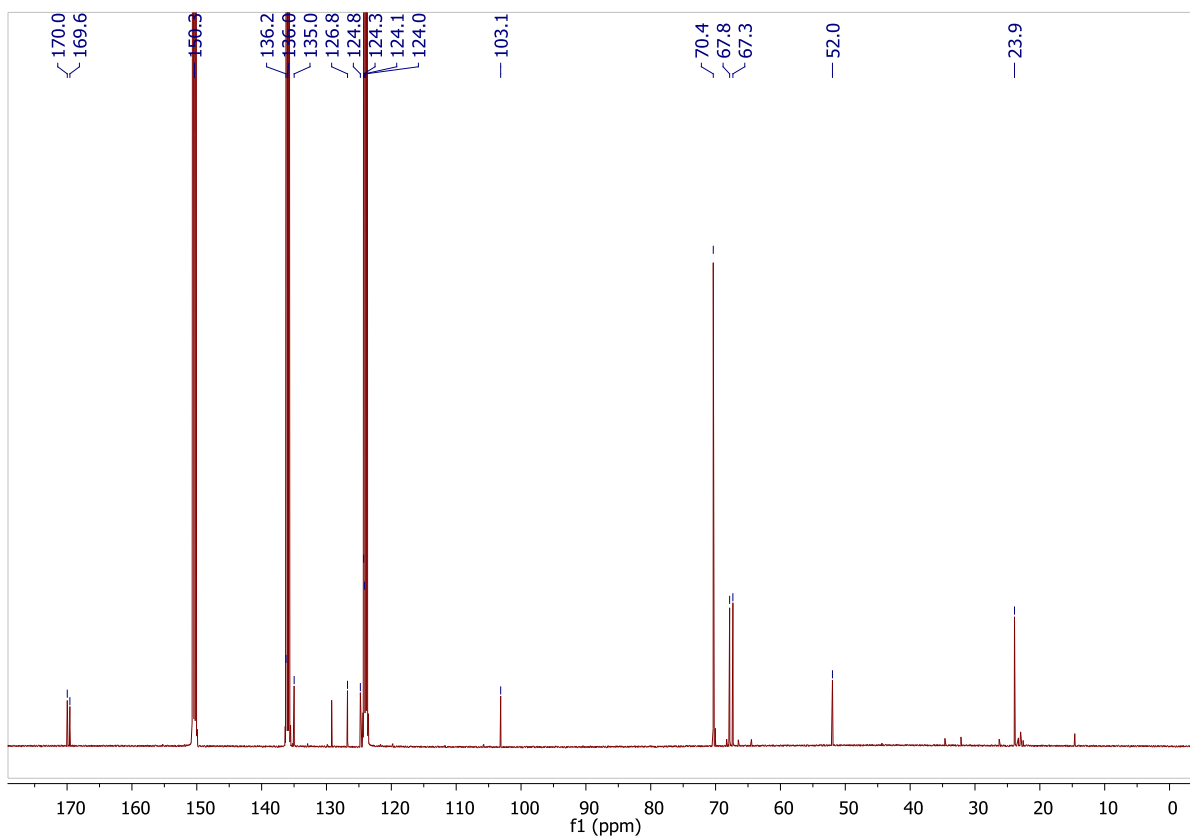
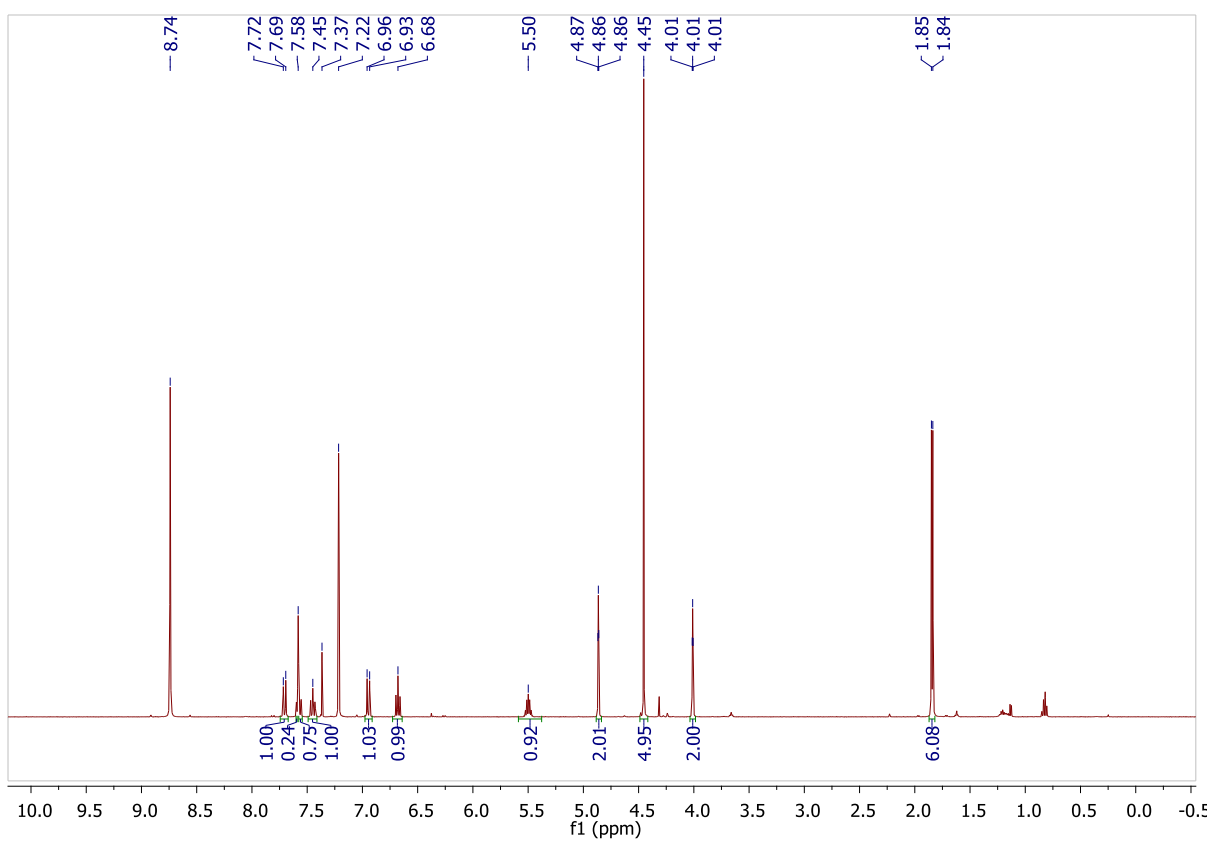


**Figure S32.** <sup>1</sup>H and <sup>13</sup>C NMR spectra of **7** in NC<sub>5</sub>D<sub>5</sub>.



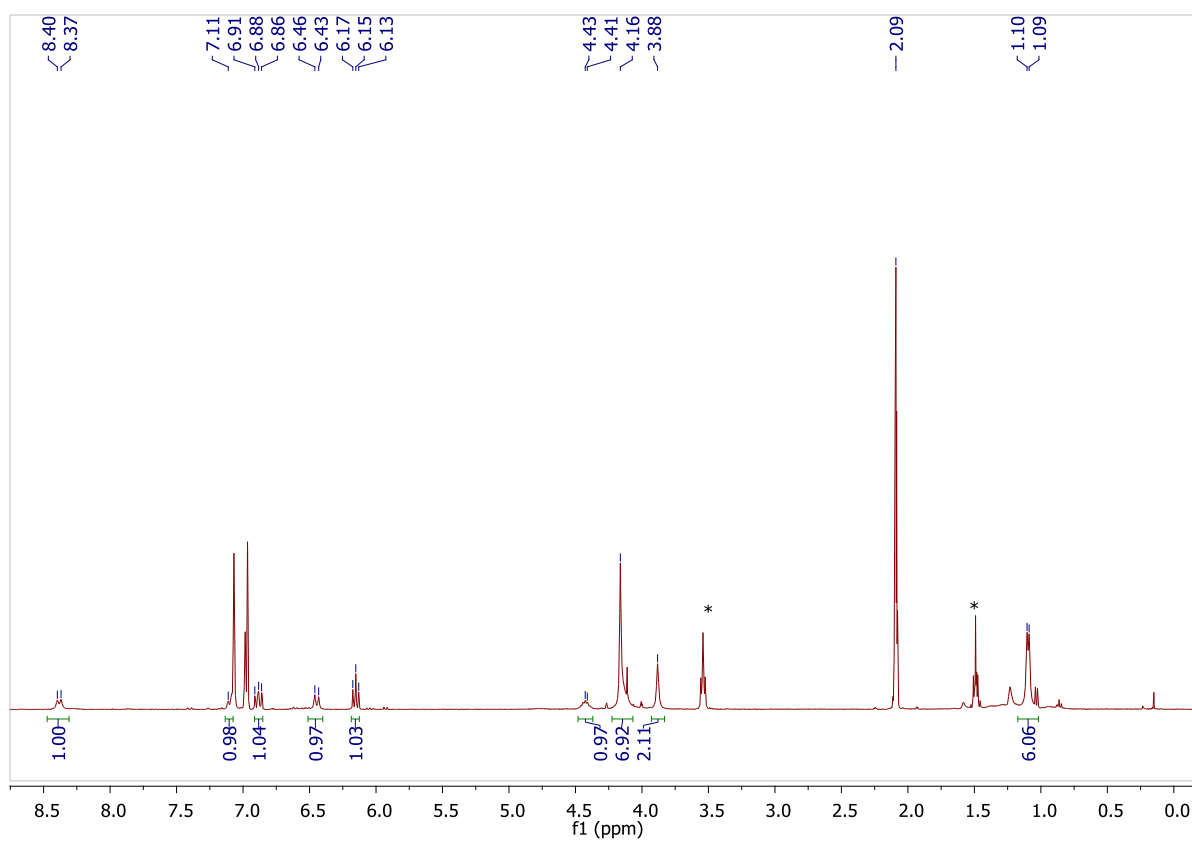


**Figure S33.**  $^1\text{H}$  NMR spectrum of **8** in  $\text{toluene-}d_8$  at 353 K; asterisks indicate resonances due to THF.

Free energies ( $G^0$ , hartree), enthalpies ( $H^0$ , hartree), and cartesian coordinates (Å) of optimized structures. Calculations were performed with the Gaussian16 program suite.<sup>1</sup>

**[H-AT<sup>Fc</sup>]<sup>+</sup> (2-ox)**

$H^0 = -909.761506$

$G^0 = -909.826358$

Fe	-2.069332	-0.021119	0.055429
C	4.391041	1.777362	0.578047
H	5.005710	2.621890	0.876694
C	5.069002	0.732877	-0.111559
H	6.135752	0.892957	-0.250383
C	4.580489	-0.430029	-0.641700
C	-0.217155	-1.213039	0.517976
C	-1.316495	-1.993222	0.000197
H	-1.269301	-2.611629	-0.886078
C	-1.685674	1.773708	-0.996316
H	-0.702733	2.219005	-1.066551
C	3.058776	1.844445	0.899650
H	2.733232	2.744916	1.414331
C	-2.416093	-1.885607	0.900103
H	-3.361915	-2.401000	0.807927
C	-0.734376	-0.480759	1.644422
H	-0.193976	0.223906	2.255537
C	-2.663877	2.054039	0.006371
H	-2.542397	2.733807	0.838720
C	3.242397	-0.981020	-0.650657
C	2.091425	-0.336290	0.056039
C	-2.059542	-0.945736	1.909954
H	-2.680788	-0.621022	2.733271
C	2.028814	0.894904	0.664970
H	1.049361	1.208839	1.008024
C	-3.810576	1.256622	-0.254097
H	-4.705875	1.216165	0.350973
C	-3.537051	0.454409	-1.399772
H	-4.203301	-0.277439	-1.835492
C	-2.225370	0.783871	-1.871143
H	-1.732502	0.353828	-2.732123
H	5.281421	-1.084383	-1.152611
O	3.004028	-2.045227	-1.248890
N	0.990677	-1.173528	-0.084893
H	1.248579	-1.933462	-0.732941

**[H-AT<sup>Fc</sup>]<sup>-</sup> (2-red)**

$H^0 = -909.998460$

$G^0 = -910.062177$

Fe	-2.031509	-0.001760	0.035784
C	4.176087	1.830937	0.616930
H	4.732340	2.710418	0.940377
C	4.902608	0.824041	0.001557
H	5.973228	1.022026	-0.093638
C	4.497238	-0.408253	-0.549303
C	-0.320782	-1.316376	0.479078
C	-1.447387	-1.988182	-0.118184

H	-1.406549	-2.543735	-1.045894
C	-1.316423	1.465692	-1.256411
H	-0.278973	1.515256	-1.556634
C	2.770894	1.851873	0.845356
H	2.365335	2.770890	1.268229
C	-2.587365	-1.846797	0.735967
H	-3.564983	-2.279511	0.569988
C	-0.837454	-0.622387	1.630291
H	-0.269810	0.024797	2.280449
C	-1.877044	2.062148	-0.083515
H	-1.335923	2.661205	0.636624
C	3.211561	-1.037193	-0.569944
C	2.005552	-0.444513	0.069476
C	-2.209529	-0.993443	1.815438
H	-2.846071	-0.663006	2.625852
C	1.840381	0.849313	0.593699
H	0.811819	1.112006	0.825835
C	-3.256752	1.696659	-0.004740
H	-3.944173	1.972420	0.783863
C	-3.548590	0.851570	-1.119122
H	-4.498382	0.377695	-1.328743
C	-2.349115	0.707253	-1.887035
H	-2.233791	0.097246	-2.773038
H	5.260040	-1.012077	-1.035262
O	3.052593	-2.151827	-1.147965
N	0.930517	-1.330592	-0.050856
H	1.197474	-2.085158	-0.685913

**[H-AT<sup>Fc/iPr</sup>] (5) (HN<sup>iPr</sup> group)**

$H^0 = -1007.959605$

$G^0 = -1008.030978$

Fe	-2.540323	-0.321911	-0.023545
N	0.633309	-0.690676	-0.385409
C	-2.685210	-1.020213	-1.959574
H	-3.494689	-0.774508	-2.633131
C	-1.475393	-0.279998	-1.807117
H	-1.202018	0.602189	-2.366596
C	1.019516	3.037469	-0.401477
H	0.248325	3.795739	-0.532842
C	-4.152163	-0.272037	1.276431
H	-4.883936	-1.063686	1.358521
C	-2.926528	-0.183827	2.004841
H	-2.568780	-0.896958	2.734390
C	4.185635	-2.821110	1.256649
H	3.583708	-2.739916	2.166371
H	5.161258	-3.239310	1.520058
H	3.691041	-3.525473	0.577467
C	-1.426550	-2.050649	-0.325572
H	-1.101375	-2.714481	0.463099
C	2.329446	3.538172	-0.235539
H	2.451446	4.616353	-0.293089

C	-4.212491	0.836830	0.378541
H	-4.999278	1.034470	-0.336139
C	4.352853	-1.454658	0.585271
H	4.834772	-0.778455	1.304069
C	-0.670510	-0.924748	-0.796212
C	-2.229857	0.980655	1.561789
H	-1.252390	1.302707	1.891889
C	0.556582	1.742340	-0.429832
H	-0.513337	1.640341	-0.560309
C	-2.658282	-2.111144	-1.038574
H	-3.449731	-2.830801	-0.881726
C	5.226262	-1.546302	-0.677256
H	4.785149	-2.251742	-1.389135
H	6.234252	-1.892736	-0.426122
H	5.307046	-0.574546	-1.171832
C	3.459315	2.787322	0.010112
H	4.386518	3.346991	0.121947
C	1.223885	0.476823	-0.289046
C	-3.024376	1.609542	0.553905
H	-2.761890	2.500673	0.000341
C	3.607893	1.394630	0.155848
H	4.623329	1.080621	0.373414
C	2.676807	0.359287	0.063415
N	3.032553	-0.923869	0.280533
H	2.246931	-1.556259	0.106039

**[H-ATI<sup>Fc/iPr</sup>] (5-isom) (HN<sup>Fc</sup> group)**

$$H^0 = -1007.955491$$

$$G^0 = -1008.026793$$

Fe	-2.528440	-0.306287	-0.009766
N	2.950368	-0.985567	0.221678
C	-2.764818	-0.986139	-1.945552
H	-3.599271	-0.724218	-2.580878
C	-1.540782	-0.259162	-1.842914
H	-1.280970	0.627763	-2.399952
C	1.121741	3.072714	-0.421228
H	0.368048	3.844280	-0.571076
C	-4.075005	-0.230557	1.364565
H	-4.815422	-1.009313	1.483826
C	-2.814857	-0.161370	2.034127
H	-2.435049	-0.879096	2.747925
C	4.084148	-2.800077	1.354275
H	3.469916	-2.648116	2.247050
H	5.051347	-3.210610	1.663754
H	3.581154	-3.536658	0.718329
C	-1.456135	-2.038247	-0.363271
H	-1.111742	-2.708096	0.412350
C	2.403705	3.517977	-0.196793
H	2.566077	4.592415	-0.200071
C	-4.160954	0.879638	0.470460
H	-4.977853	1.089932	-0.205717
C	4.265402	-1.481453	0.593024
H	4.787756	-0.779705	1.264449
C	-0.722396	-0.913238	-0.862563
C	-2.121072	0.990816	1.556190
H	-1.122675	1.296185	1.835280

C	0.620704	1.755154	-0.502020
H	-0.443323	1.687626	-0.690917
C	-2.710181	-2.087652	-1.040508
H	-3.497992	-2.805545	-0.861718
C	5.127492	-1.684416	-0.665792
H	4.632324	-2.385822	-1.345388
H	6.111251	-2.089359	-0.405002
H	5.272030	-0.741980	-1.202823
C	3.541871	2.707831	0.036329
H	4.474749	3.254934	0.166561
C	1.257550	0.532107	-0.344829
C	-2.952995	1.631834	0.587214
H	-2.700512	2.516301	0.018720
C	3.661888	1.344114	0.133270
H	4.671510	0.995345	0.321274
C	2.690644	0.277594	0.031809
N	0.591375	-0.643793	-0.478829
H	1.210184	-1.422084	-0.216746

**[H-ATI<sup>Fc/iPr</sup>]<sup>+</sup> (5-ox)**

$$H^0 = -1007.758885$$

$$G^0 = -1007.834232$$

Fe	-2.647215	-0.363023	-0.069864
N	0.679594	-0.670407	-0.059235
C	-2.406746	-1.151951	-1.956192
H	-3.113972	-0.986260	-2.757590
C	-1.268938	-0.341706	-1.670483
H	-0.964241	0.525310	-2.237846
C	1.103461	3.061289	-0.294203
H	0.319856	3.808930	-0.398940
C	-4.451308	-0.330615	1.030976
H	-5.122711	-1.175089	1.098606
C	-3.361224	-0.051432	1.915656
H	-3.054691	-0.657386	2.756807
C	4.409420	-2.725609	1.309957
H	3.873100	-2.597005	2.254427
H	5.404473	-3.119595	1.530281
H	3.882178	-3.472426	0.705083
C	-1.352592	-2.033238	-0.106495
H	-1.111302	-2.649863	0.747928
C	2.402090	3.553578	-0.238745
H	2.526172	4.629019	-0.321964
C	-4.489687	0.700392	0.044864
H	-5.189236	0.774873	-0.775797
C	4.526985	-1.400195	0.553255
H	5.047350	-0.681752	1.198120
C	-0.505926	-0.962635	-0.595550
C	-2.739290	1.151969	1.483197
H	-1.859010	1.602526	1.920969
C	0.646423	1.743013	-0.246902
H	-0.432695	1.641775	-0.300754
C	-2.461872	-2.198069	-0.983717
H	-3.223921	-2.961721	-0.910445
C	5.296366	-1.556786	-0.766580
H	4.804018	-2.294750	-1.407565
H	6.316456	-1.898580	-0.569503

H	5.351046	-0.613129	-1.316639
C	3.566017	2.796328	-0.079223
H	4.494460	3.362436	-0.063492
C	1.320482	0.512852	-0.114514
C	-3.420942	1.606744	0.320046
H	-3.166348	2.478968	-0.266273
C	3.727407	1.425640	0.074791
H	4.757503	1.108738	0.188604
C	2.780711	0.376382	0.101586
N	3.172910	-0.886090	0.311439
H	2.396539	-1.546641	0.286680

**[H-ATI<sup>Fc/iPr</sup>]<sup>-</sup> (5-red)**

$$H^0 = -1007.968676$$

$$G^0 = -1008.041553$$

Fe	2.527655	-0.324666	0.015572
N	-0.719734	-0.685977	-0.211557
C	2.338823	-1.494361	1.682703
H	3.029279	-1.466380	2.516284
C	1.160070	-0.695666	1.543430
H	0.805810	0.034379	2.255417
C	-1.219738	2.950245	0.744563
H	-0.484784	3.633139	1.177754
C	4.292620	0.054875	-1.006771
H	5.043085	-0.694702	-1.220603
C	3.162224	0.370395	-1.824377
H	2.902666	-0.107611	-2.759296
C	-4.641517	-2.774496	-0.862037
H	-5.046026	-2.515058	-1.845485
H	-5.406954	-3.313243	-0.290494
H	-3.796914	-3.458558	-1.015810
C	1.354269	-2.000807	-0.338023
H	1.158548	-2.417568	-1.316748
C	-2.466999	3.494504	0.526361
H	-2.605464	4.537934	0.810108
C	4.223227	0.865582	0.169501
H	4.912833	0.839093	1.002778
C	-4.176144	-1.513493	-0.126589
H	-5.046782	-0.856537	0.009122
C	0.489441	-1.042877	0.306680
C	2.396019	1.377651	-1.161842
H	1.444940	1.779097	-1.482099
C	-0.707958	1.645805	0.504599
H	0.338689	1.517489	0.744229
C	2.460975	-2.305820	0.512616
H	3.265752	-2.995844	0.293820
C	-3.613993	-1.851244	1.266127
H	-2.743437	-2.510017	1.174901
H	-4.365666	-2.344829	1.896708
H	-3.282857	-0.936509	1.766147
C	-3.594351	2.838531	-0.054887
H	-4.493194	3.439278	-0.188426
C	-1.344230	0.489408	-0.027404
C	3.050322	1.676594	0.073818
H	2.690493	2.366053	0.825344
C	-3.665237	1.522457	-0.500693

H	-4.620375	1.239080	-0.946735
C	-2.745826	0.462402	-0.488051
N	-3.216923	-0.795998	-0.986135
H	-2.374053	-1.371674	-1.066287

**[Bi(ATI<sup>Fc/iPr</sup>)<sub>3</sub>] (trans-8)**

$$H^0 = -3027.615368$$

$$G^0 = -3027.782415$$

Bi	0.307541	-0.996097	-0.262857
Fe	4.550081	1.916633	0.548587
Fe	-2.546113	3.396029	0.866769
Fe	-4.614002	-1.553198	-1.140799
N	-0.484596	1.292379	-0.643747
C	0.649808	4.336456	-3.898497
H	0.814913	5.258426	-4.448981
C	0.840250	3.129265	-4.583156
H	1.109406	3.222994	-5.634546
N	-1.845410	-1.663137	0.602661
N	1.564341	-3.150892	0.128699
C	0.757018	1.826781	-4.131291
C	-1.105026	1.860583	0.489829
N	2.715958	-0.703515	-0.198189
N	0.597539	-0.075318	-2.653494
N	0.181705	-0.805644	2.091565
C	-2.335136	1.346923	1.008242
H	-2.945803	0.629144	0.488697
C	4.208562	2.442556	-1.419919
H	4.881828	3.054527	-2.003895
C	0.701266	-2.409273	-3.436863
H	1.205698	-2.796138	-2.547050
H	0.995207	-3.047559	-4.276769
H	-0.379153	-2.507178	-3.295062
C	-6.362413	-1.095122	-0.108308
H	-6.736534	-1.647071	0.743033
C	-3.201814	4.304180	-0.886564
H	-2.894481	3.995121	-1.875097
C	-1.920120	-1.690527	5.072141
H	-1.564413	-1.828622	6.092157
C	4.255523	1.021963	-1.318909
H	4.953237	0.373957	-1.826037
C	5.963104	-2.577283	-0.217424
H	6.941437	-2.172887	0.039717
C	5.298381	3.334505	1.857571
H	5.004112	4.374740	1.842259
C	1.104821	-0.956557	-3.712750
C	4.645569	2.290369	2.580231
H	3.774337	2.405835	3.208285
C	-3.305933	-1.710300	4.911423
H	-3.913143	-1.802343	5.807534
C	0.250556	4.432273	-2.577430
H	0.137878	5.443212	-2.186700
C	-2.575521	1.917242	2.290986
H	-3.426471	1.715704	2.925886
C	0.092539	-4.425213	1.632994
H	0.720053	-4.109018	2.469663
H	-0.295051	-5.426645	1.848909

H	-0.755233	-3.743459	1.562118
C	-0.623450	2.823056	1.448111
H	0.265319	3.429846	1.354857
C	-3.962857	-1.652174	3.686948
H	-5.051315	-1.668549	3.724134
C	2.634901	-0.849706	-3.846475
H	2.952013	0.183251	-4.009091
H	2.993350	-1.462566	-4.680823
H	3.112104	-1.205288	-2.929445
C	2.560462	1.781782	0.045053
H	1.751447	1.810876	0.755999
C	-3.665527	-3.223875	-0.317668
H	-3.966419	-3.751598	0.574780
C	-3.428497	-1.630905	2.403145
H	-4.166261	-1.658704	1.609794
C	5.953398	-3.865293	-0.736017
H	6.910647	-4.354104	-0.894385
C	6.365570	2.753317	1.107985
H	7.024298	3.275927	0.428494
C	0.893137	-4.448710	0.324320
H	1.657598	-5.229726	0.434728
C	-2.524913	5.254993	-0.062507
H	-1.629817	5.801109	-0.325293
C	-2.723409	-2.136730	-0.370478
C	0.472545	1.226531	-2.855018
C	-0.037516	2.019893	-1.694248
C	-1.521545	2.839952	2.559539
H	-1.429300	3.468653	3.434486
C	2.273738	-1.611884	3.268854
H	1.825120	-2.144049	4.111402
H	3.258055	-1.256268	3.591529
H	2.412434	-2.323392	2.453043
C	3.202410	0.592733	-0.436650
C	5.311441	1.062454	2.282666
H	5.035877	0.083899	2.649533
C	-2.644015	-1.716275	-1.745410
H	-2.063261	-0.878882	-2.109890
C	-0.052317	3.429194	-1.651983
H	-0.379389	3.821154	-0.702565
C	-0.906409	-1.487821	4.144775
H	0.077815	-1.505297	4.584773
C	4.907651	-1.683806	-0.033194
H	5.208745	-0.699679	0.299897
C	3.157940	2.913801	-0.580750
H	2.879601	3.944884	-0.420489
C	-0.012545	-4.828646	-0.859029
H	-0.810499	-4.091787	-0.994768
H	-0.487059	-5.798429	-0.674613
H	0.547400	-4.896651	-1.795913
C	-3.484259	-2.563970	-2.526488
H	-3.654745	-2.478925	-3.590563
C	-6.649793	-1.373053	-1.478787
H	-7.268357	-2.179560	-1.847407
C	-0.906730	-1.229115	2.741000
C	1.285548	0.709718	3.813554
H	0.762115	1.559141	3.370149
H	2.282061	1.036796	4.126544

H	0.739821	0.414313	4.710752
C	-2.104303	-1.548759	1.909181
C	4.799708	-4.573670	-1.089497
H	4.962627	-5.537657	-1.569383
C	-4.116482	-3.490360	-1.644168
H	-4.844509	-4.239688	-1.923063
C	3.510320	-1.792759	-0.207828
C	-5.470448	0.018794	-0.060469
H	-5.063217	0.469636	0.831720
C	1.441739	-0.413120	2.773811
H	2.051612	0.019509	1.980759
C	6.374278	1.350519	1.371047
H	7.052795	0.631251	0.933308
C	3.469559	-4.250172	-0.883118
H	2.774128	-5.002927	-1.237268
C	-3.214952	5.335433	1.184010
H	-2.925507	5.938711	2.033313
C	-5.926623	-0.436344	-2.278858
H	-5.900229	-0.411169	-3.359402
C	-4.319280	4.432144	1.132098
H	-5.013116	4.229175	1.936245
C	2.823406	-3.115721	-0.282864
C	-4.312436	3.797258	-0.146680
H	-5.007864	3.039216	-0.475034
C	-5.190043	0.417649	-1.402921
H	-4.500394	1.195083	-1.699163
H	0.645146	-0.691696	-4.677270
H	0.974465	1.103211	-4.906105

**[Bi(ATI<sup>Fe/Pr</sup>)<sub>3</sub>] (*cis*-8)**

$$H^0 = -3027.608795$$

$$G^0 = -3027.775106$$

Bi	0.016848	0.122797	1.437342
Fe	2.762446	-2.340522	-2.394055
Fe	-4.267682	-1.263503	-1.489635
Fe	1.229538	3.606947	-2.212331
N	-1.567568	-1.360152	0.393984
C	-1.522970	-5.941842	0.210910
H	-1.669741	-6.973530	-0.096535
C	-1.076611	-5.713905	1.519815
H	-0.969285	-6.601211	2.142357
N	-0.538286	1.909245	-0.046920
N	2.157700	1.315031	2.088960
C	-0.724070	-4.532496	2.142235
C	-2.423026	-0.754651	-0.556162
N	2.064030	-0.735871	0.388281
N	-0.051411	-2.229754	2.421836
N	-1.724316	1.563477	2.290743
C	-3.498524	0.109939	-0.166751
H	-3.844401	0.235185	0.845335
C	1.493581	-3.773437	-1.630057
H	1.545029	-4.826228	-1.868784
C	0.988449	-1.350724	4.478642
H	1.601004	-0.614588	3.950763
H	1.530501	-1.632170	5.387230
H	0.050056	-0.875440	4.781888

C 0.387287 5.467676 -2.609893  
 H -0.636224 5.630743 -2.918311  
 C -4.976011 -3.115329 -0.852076  
 H -4.482408 -3.728064 -0.112959  
 C -4.459925 3.864095 1.141550  
 H -5.409538 4.032402 1.647578  
 C 2.159785 -3.134041 -0.546066  
 H 2.793523 -3.615547 0.182878  
 C 5.688493 -1.339260 1.132970  
 H 6.342134 -2.004969 0.569839  
 C 3.281011 -2.452202 -4.394655  
 H 2.594851 -2.764916 -5.169624  
 C 0.729423 -2.588257 3.613628  
 C 3.449485 -1.118109 -3.914368  
 H 2.906910 -0.249271 -4.255921  
 C -4.245717 4.618610 -0.012374  
 H -5.018086 5.324803 -0.303623  
 C -1.815026 -4.945839 -0.704130  
 H -2.156740 -5.281942 -1.682269  
 C -4.009349 0.764635 -1.323952  
 H -4.820419 1.478308 -1.341598  
 C 1.275881 3.608805 2.209597  
 H 1.570050 3.739248 1.165811  
 H 1.383454 4.567330 2.729342  
 H 0.220998 3.327773 2.225686  
 C -2.320295 -0.666917 -1.987056  
 H -1.622894 -1.210473 -2.604182  
 C -3.109067 4.535860 -0.807003  
 H -3.072924 5.218582 -1.655287  
 C 2.061996 -3.258410 3.230942  
 H 1.896885 -4.138588 2.604277  
 H 2.608381 -3.569402 4.127867  
 H 2.690717 -2.558524 2.674338  
 C 0.989971 -1.523954 -1.715458  
 H 0.615818 -0.564396 -2.035391  
 C -0.117919 2.041518 -2.590109  
 H -1.128007 2.128914 -2.958868  
 C -2.009472 3.686803 -0.717539  
 H -1.295492 3.829824 -1.512882  
 C 6.251669 -0.746323 2.257473  
 H 7.274292 -1.010430 2.511618  
 C 4.125665 -3.309524 -3.626623  
 H 4.195814 -4.384346 -3.719965  
 C 2.140902 2.543030 2.897760  
 H 3.161919 2.948302 2.953339  
 C -4.728792 -3.140101 -2.258711  
 H -4.028112 -3.785688 -2.769330  
 C 0.265902 2.008569 -1.202503  
 C -0.662646 -3.162693 1.708737  
 C -1.367367 -2.697158 0.477474  
 C -3.286654 0.274767 -2.452121  
 H -3.460584 0.540158 -3.486048  
 C -3.331807 0.174182 3.648360  
 H -4.270207 0.607950 3.292252  
 H -3.499731 -0.193148 4.666457  
 H -3.087307 -0.680440 3.010403  
 C 1.834789 -1.732163 -0.575283

C 4.401106 -1.147691 -2.850934  
 H 4.712252 -0.305835 -2.249222  
 C 1.697361 1.891773 -1.167573  
 H 2.285139 1.866083 -0.265714  
 C -1.772000 -3.556008 -0.562277  
 H -2.123963 -3.028688 -1.434668  
 C -3.636616 2.941439 1.768663  
 H -4.071625 2.530953 2.667389  
 C 4.399142 -1.244036 0.618741  
 H 4.238305 -1.849229 -0.260349  
 C 0.765364 -2.780283 -2.350535  
 H 0.182885 -2.944774 -3.246347  
 C 1.640469 2.295212 4.332423  
 H 0.609067 1.931075 4.314762  
 H 1.656170 3.224953 4.911386  
 H 2.247150 1.553083 4.858648  
 C 2.180416 1.816903 -2.503696  
 H 3.217672 1.741136 -2.795584  
 C 1.492351 5.228997 -3.481420  
 H 1.449028 5.163711 -4.559701  
 C -2.350147 2.398103 1.468298  
 C -2.356819 2.356203 4.622020  
 H -1.518096 3.053550 4.541363  
 H -2.383914 1.969621 5.646302  
 H -3.276952 2.919753 4.457405  
 C -1.633682 2.662524 0.182069  
 C 5.595114 0.167896 3.081071  
 H 6.164303 0.523122 3.939235  
 C 1.060302 1.916024 -3.383991  
 H 1.094658 1.928285 -4.464839  
 C 3.236671 -0.530664 1.008008  
 C 0.865042 5.423236 -1.263694  
 H 0.263071 5.523104 -0.372091  
 C -2.166901 1.183126 3.642151  
 H -1.310366 0.623722 4.043800  
 C 4.818370 -2.503395 -2.674096  
 H 5.517988 -2.864312 -1.932829  
 C 4.326208 0.719363 2.972736  
 H 4.107330 1.422650 3.765487  
 C -5.543558 -2.140718 -2.870847  
 H -5.558550 -1.887832 -3.921967  
 C 2.654108 5.035304 -2.674340  
 H 3.644410 4.792336 -3.033875  
 C -6.292764 -1.494090 -1.841068  
 H -6.969524 -0.661521 -1.975373  
 C 3.245560 0.546633 2.048542  
 C -5.940228 -2.096104 -0.594661  
 H -6.306641 -1.801276 0.378863  
 C 2.265701 5.153414 -1.304955  
 H 2.911795 5.020031 -0.448734  
 H 0.156345 -3.283972 4.245669  
 H -0.397076 -4.673780 3.165281

**[Bi(AT<sup>Fe</sup>)<sub>3</sub>]<sup>+</sup> (4<sup>+</sup>)**

$H^0 = -2733.501477$

$G^0 = -2733.648408$



H	0.705704	5.528557	-4.025800	C	5.866954	-4.258757	0.072725
C	0.463616	3.434161	-4.365966	H	6.753277	-4.861384	0.250127
H	0.537179	3.621765	-5.435598	C	6.485061	2.839328	1.067773
N	-1.824051	-1.576951	0.496802	H	7.288323	3.212354	0.448273
N	1.579278	-3.287568	-0.033909	C	0.855066	-4.571859	0.010881
C	0.352443	2.105829	-4.019830	H	1.572658	-5.400589	0.082847
C	-1.178334	1.820593	0.675781	C	-2.381832	5.312098	0.272025
N	2.874241	-0.829959	-0.307807	H	-1.454464	5.836597	0.090838
N	0.467114	0.117217	-2.649513	C	-2.696023	-2.024189	-0.508769
N	0.198136	-0.805344	2.005486	C	0.278962	1.417492	-2.755480
C	-2.457554	1.337452	1.098614	C	-0.106485	2.119188	-1.498612
H	-3.082652	0.691217	0.505558	C	-1.640188	2.681785	2.783005
C	4.753296	1.946757	-1.761902	H	-1.563207	3.250565	3.699187
H	5.541482	2.413120	-2.337312	C	2.292524	-1.677599	3.107220
C	0.651881	-2.171504	-3.532839	H	1.874220	-2.149054	3.999605
H	1.263764	-2.528903	-2.698568	H	3.319563	-1.380752	3.346013
H	0.919054	-2.764999	-4.412784	H	2.325910	-2.424654	2.313214
H	-0.400396	-2.363524	-3.302799	C	3.437475	0.303393	-0.721719
C	-6.372146	-1.345135	-0.018628	C	5.179547	1.437670	2.360772
H	-6.665562	-2.016578	0.776550	H	4.790963	0.555374	2.850589
C	-3.055806	4.452496	-0.648324	C	-2.689196	-1.458953	-1.833032
H	-2.718441	4.201520	-1.643201	H	-2.192145	-0.542087	-2.119973
C	-1.846945	-1.824274	4.988330	C	0.025309	3.503373	-1.312123
H	-1.483200	-1.919812	6.009571	H	-0.168343	3.825131	-0.300586
C	4.732576	0.585120	-1.336601	C	-0.861033	-1.499630	4.065318
H	5.491809	-0.148913	-1.559457	H	0.113884	-1.396382	4.513069
C	5.860625	-2.977311	0.560572	C	4.892366	-1.958920	0.361116
H	6.743824	-2.662875	1.112842	H	5.209198	-0.974183	0.692430
C	5.341378	3.573576	1.498717	C	3.579760	2.586411	-1.262612
H	5.112671	4.601195	1.253853	H	3.301002	3.622449	-1.392625
C	0.904149	-0.685177	-3.800606	C	-0.004339	-4.786499	-1.243243
C	4.529158	2.699498	2.284097	H	-0.765599	-4.006135	-1.339543
H	3.571999	2.943640	2.723242	H	-0.523973	-5.747546	-1.178640
C	-3.217429	-2.018462	4.817761	H	0.599753	-4.787113	-2.155022
H	-3.809073	-2.208757	5.708261	C	-3.482110	-2.290583	-2.677860
C	0.333426	4.567968	-2.175953	H	-3.698950	-2.109012	-3.720936
H	0.391167	5.536897	-1.682466	C	-6.691707	-1.497239	-1.400992
C	-2.729596	1.843072	2.402054	H	-7.255035	-2.310364	-1.836782
H	-3.626175	1.665082	2.978642	C	-0.878981	-1.262999	2.663052
C	-0.003986	-4.601251	1.281890	C	1.425022	0.662399	3.710148
H	0.604409	-4.408401	2.169727	H	0.805038	1.489370	3.363335
H	-0.474163	-5.583460	1.392172	H	2.440423	1.033742	3.889266
H	-0.793641	-3.848928	1.236485	H	1.032802	0.331573	4.673043
C	-0.687228	2.679671	1.719274	C	-2.060128	-1.596583	1.825123
H	0.244619	3.227631	1.710590	C	4.837934	-4.847769	-0.714145
C	-3.877861	-2.004822	3.595720	H	5.097824	-5.779945	-1.211910
H	-4.954401	-2.161367	3.630485	C	-4.002073	-3.356023	-1.884875
C	2.392646	-0.442795	-4.107175	H	-4.675161	-4.130997	-2.223922
H	2.600683	0.617067	-4.276767	C	3.600738	-1.995369	-0.143500
H	2.699688	-1.001537	-4.996977	C	-5.578172	-0.167215	0.124419
H	3.002243	-0.779982	-3.263462	H	-5.174297	0.216570	1.049332
C	2.845095	1.615892	-0.526329	C	1.490344	-0.446655	2.644392
H	1.921672	1.797414	-0.000346	H	2.071366	-0.018765	1.822888
C	-3.527710	-3.197170	-0.550211	C	6.378175	1.513453	1.596769
H	-3.750265	-3.845271	0.283972	H	7.084404	0.710367	1.437867
C	-3.357639	-1.856012	2.312795	C	3.557021	-4.412445	-0.899791
H	-4.095760	-1.929745	1.524329	H	2.936168	-5.024555	-1.547629



C	-3.133342	5.342704	1.484229	H	-4.939022	3.257289	-0.419281
H	-2.866523	5.877152	2.385250	C	-5.392274	0.399548	-1.172743
C	-6.087085	-0.418536	-2.114138	H	-4.791678	1.267398	-1.404026
H	-6.111987	-0.272827	-3.184989	H	0.313341	-0.424948	-4.691547
C	-4.272450	4.500309	1.314780	H	0.352665	1.435976	-4.871787
H	-5.018203	4.281113	2.066160				
C	2.849293	-3.270448	-0.318694				
C	-4.225218	3.952364	-0.002260				

## References

- 1 Gaussian 16, Revision A.03, M. J. Frisch, G. W. Trucks, H. B. Schlegel, G. E. Scuseria, M. A. Robb, J. R. Cheeseman, G. Scalmani, V. Barone, G. A. Petersson, H. Nakatsuji, X. Li, M. Caricato, A. V. Marenich, J. Bloino, B. G. Janesko, R. Gomperts, B. Mennucci, H. P. Hratchian, J. V. Ortiz, A. F. Izmaylov, J. L. Sonnenberg, D. Williams-Young, F. Ding, F. Lipparini, F. Egidi, J. Goings, B. Peng, A. Petrone, T. Henderson, D. Ranasinghe, V. G. Zakrzewski, J. Gao, N. Rega, G. Zheng, W. Liang, M. Hada, M. Ehara, K. Toyota, R. Fukuda, J. Hasegawa, M. Ishida, T. Nakajima, Y. Honda, O. Kitao, H. Nakai, T. Vreven, K. Throssell, J. A. Montgomery, Jr., J. E. Peralta, F. Ogliaro, M. J. Bearpark, J. J. Heyd, E. N. Brothers, K. N. Kudin, V. N. Staroverov, T. A. Keith, R. Kobayashi, J. Normand, K. Raghavachari, A. P. Rendell, J. C. Burant, S. S. Iyengar, J. Tomasi, M. Cossi, J. M. Millam, M. Klene, C. Adamo, R. Cammi, J. W. Ochterski, R. L. Martin, K. Morokuma, O. Farkas, J. B. Foresman and D. J. Fox, Gaussian, Inc., Wallingford CT, 2016.